DOI: 10.2478/ata-2019-0001

Acta Technologica Agriculturae 1
Nitra, Slovaca Universitas Agriculturae Nitriae, 2019, pp. 1–4

EFFECT OF DIFFERENT RATIOS OF BIOMATERIALS TO BANANA PEELS ON THE WEIGHT LOSS OF BIODEGRADABLE POTS

Siti Nor Amirah MOHD RAFEE, Yit Leng LEE*, Mohd Riduan JAMALLUDIN, Norawanis ABDUL RAZAK, Nur lailina MAKHTAR, Ras Izzati ISMAIL

Universiti Malaysia Perlis, Kampus Uniciti Alam, Perlis, Malaysia

The present study was undertaken to determine the weight loss of pots made of different ratios of biomaterials and banana peels. Two types of biodegradable pots were produced using different ratios of biomaterials (B) and banana peels (BP). The ratios of B to BP tested in this study were B50% : BP50% and B30% : BP 70%. The weight loss of biodegradable pot with ratio B30% : BP70% was significantly higher than biodegradable pot with ratio B50% : BP50% after the empty biodegradable pots were left to decompose on the ground for 60 days. This result suggests that higher content of banana peels increase the microbial decomposition of the biodegradable pot. On the contrary, the weight loss of biodegradable pot with ratio B50%:BP50% was higher when they were filled with soil and left to decompose on the ground for 60 days. This is probably due to the lower content of banana peels, what decreased the tensile strength of biodegradable pot filled with soil, making it highly decomposable in such manner. In terms of degradability, biodegradable pot with ratio B30% : BP70% is more appropriate than pot with ratio B50% : BP50%.

Keywords: decomposition; carbon; nitrogen; pot; glycerol; soil

Non-renewable petroleum-based plastic items are widely used in agriculture and plastic waste accumulation imposes pollution problems to environment. Degradation of plastic waste in landfills takes more than 20 years and plastic waste cannot be conventionally recycled due to high level of ash, impurities and heavy metals (Webb et al., 2013). In nursery and floriculture, plastic pots are frequently used for growing plants as they are lightweight, inexpensive, and durable. However, plastic pots are made of inert material and thus non-biodegradable. Plastic pot wastes are often burned or abandoned in the open, buried in soil, as well as disposed of in landfills. Inappropriate disposal of the plastic pot waste causes soil and water contamination, release of harmful substances and air pollutants, as well as soil quality degradation (Briassoulis et al., 2013).

An alternative way of plastic pot usage reduction is to generate biodegradable pots made of plasticizer (glycerol) and solid wastes. Uncountable amount of solid waste has been generated by agricultural production system. Landfills, incineration and environmental dumping have been primary methods for disposal of agricultural solid wastes. Banana is native to regions of Southeast Asia and cultivated throughout the tropics. In Malaysia, banana is the second most widely cultivated fruit, covering approximately 26,000 ha with a total production of 530,000 metric tonnes (Tock et al., 2010). Banana peel waste is normally disposed of in municipal landfills, contributing to existing environmental issues. An alternative management of banana waste is to use it as a fibre ingredient in combination with plasticizer in order to produce a novel product – pot made of bio-material. Compared with a plastic pot non-degradability, such bio-material pots can be broken down quickly. It was reported that the biomaterial containing less than 50% of dry matter is easier to be decomposed by the microorganisms (Kažimírová et al., 2018). Biomaterial pots are more environmentally friendly and economically attractive alternative to traditional plastic pots. Moreover, these biodegradable pots can minimize root injury by proper burying of the biomaterial pot into soil together with the seedlings.

Liew and Khor (2015) observed that bioplastic pot made of material with higher content of tapioca starch showed weight loss of approx. 24.9% in 15 day. Biomaterial in bioplastic pots helps to increase their strength. Biomaterial made of keratin with 2% of glycerol has the best mechanical and thermal properties (Ramakrishnan et al., 2018). Composition of plastic film affects the biodegradability rate. Literature on this matter reports that the plastic film decomposes at slower rate with the increasing of glycerol content (Ramakrishnan et al., 2018). Nevertheless, there is a scarcity of information on the effect of various concentrations of biomaterial and banana peels mixture on the weight loss of biodegradable pots. Aim of this study was to determine the weight loss of biodegradable pots made of different ratios of biomaterials and banana peels.

Contact address: Yit Leng Lee, Universiti Malaysia Perlis, Faculty of Engineering Technology, Department of Mechanical Engineering Technology, Kampus Uniciti Alam, Padang Besar, 02100 Perlis, Malaysia, e-mail: yllee@unimap.edu.my

Material and methods

Samples collection and preparation

Biomaterials used for the production of biodegradable pots were banana peels, tapioca starch, glycerol with 99.5% concentration and vinegar. Approximately 8 kg of banana peels were collected from a fruit stall in Perlis. Banana peels were sun-dried for 3 days and subsequently cut and blended into powder form prior to the production of biodegradable pots.

Production of biodegradable pots

Biomaterials for the production of biodegradable pots were tapioca starch, water, vinegar and glycerol using the method proposed by Liew and Khor (2015). Appropriate amounts of materials for biodegradable pots were weighed on the basis of ratio of biomaterial to banana peels. Ratios of bio-materials (B) to banana peels (BP) tested in this study were B50% : BP50% and B30% : BP 70%. Experiment for each variant was replicated three times. The tapioca starch, water, vinegar and glycerol were added and properly mixed together at room temperature. Mixture was stirred approximately for 2 minutes until it was well-mixed. Then, mixture was heated using hot plate VELP/ITALY at 55 °C until fully sticky gel texture was obtained. Afterwards, sample was poured into a tray covered with aluminium foil and spread out evenly in the tray. Subsequently, it was oven-dried at 70 °C.

Drying time of the spread varied according to individual mixture ratios. Purpose of drying the spread was to enable easier removal from aluminium foil. Then, the spread of biomaterials and banana peels was removed from aluminium foil and formed by means of plastic pot mould. Formed biodegradable pots were oven-dried at 70 °C for 24 h in order to achieve equilibrium with temperature and humidity of the surrounding. Dimensions of biodegradable pot were 9.0 cm height, 7.2 cm diameter and 0.2 cm thickness (Fig. 1).

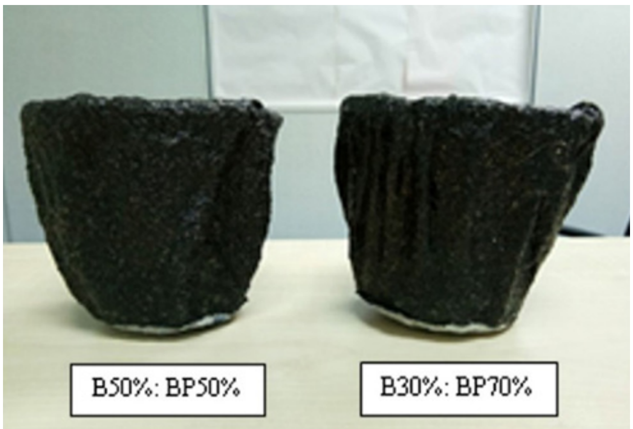

Fig. 1 Biodegradable pots with dimension of 9.0 cm height, 7.2 cm diameter and 0.2 cm thickness

Testing of biodegradable pots

Decomposition study of biodegradable pots

Degradability of pots was determined using the biodegradable pots filled with and without soil. Three biodegradable pots of each ratio were tested on the ground in order to test the degradability of the pot with soil contact. Initial oven-dried weight of biodegradable pots was taken prior to decomposition study. Biodegradable pots were collected after 3 months-long decomposition on the ground and cleaned from all impurities. Subsequently, they were oven-dried at 70 °C until a constant weight was obtained. Final weight of each dried biodegradable pot was taken. Weight loss percentages of pots were calculated by using the following formula:

$$weight\ loss\ (\%) = \frac{W_i - W_f}{W_i} \times 100 \qquad (1)$$

where:
W_i – initial oven-dried weight (g)
W_f – final oven-dried weight (g)

Total carbon and nitrogen analysis

Elemental contents of total carbon and nitrogen of the biodegradable pots at different ratios were determined using LECO CNS analyser. Analyses were performed three times.

Statistical analysis

A pair *t*-test was used to detect significant differences between weight loss percentages and contents of carbon, nitrogen and sulphur in biodegradable pots made of 50%B:50%BP and 30%B:70%BP. Statistical Analysis System (SAS) software version 9.2 was used for the statistical analysis.

Results and discussion

Decomposition of empty biodegradable pots on the ground

Disposal of plastic waste in the environment is considered to be a big problem due to its very low biodegradability and presence in large quantities (Patil, 2015). Biomaterial made of starch rather than fossil fuel plastics can decompose faster in soil and reduce environmental pollution. Table 1 shows weight loss percentages in both variants of biodegradable pots – B50% : BP50% and B30% : BP70% – over 60 days, during decomposition on the ground. The weight losses in biodegradable pot B50% : BP50% and biodegradable pot B30% : BP70% did not differ significantly after decomposing on the ground after 20 days. Weight losses of both biodegradable pots (25–26.37%) were consistent with the weight loss of bioplastic pot obtained by Liew and Khor (2015), who also produced biodegradable pots using 75% tapioca starch. Initial rapid degradation of the readily degradable material made of starch and banana peels has also been observed by Cai et al. (2018). Weight losses percentages of both pots increased after 40 days

Table 1 Weight loss percentages in biodegradable pots made of different ratios of biomaterials and banana peels (pots without soil medium)

Pots made of different ratios of biomaterials (B): banana peels (BP)	Weight loss percentages over days (%)		
	20 days	40 days	60 days
B50% : BP50%	26.37^{a} ± 0.66	31.06^{a} ±2.15	35.86^{b} ±4.60
B30% : BP70%	25.00^{a} ±0.12	30.31^{a} ±3.74	39.38^{a} ±3.14

Different letters in the same column indicate significant differences observed in independent *t*-test at α = 0.05 and ± indicate standard error (n = 3)

(30.06–31.31%). Weight loss in biodegradable pot with ratio B30% : BP70% was significantly higher (39.38%) than in biodegradable pot with ratio B50% : BP50% (35.86%) after 60 days of decomposing on the ground. This result indicates that the higher content of banana peels accelerates the microbial decomposition in the biodegradable pot. High content of carbohydrate in banana peels (Vu et al., 2017) increases the decomposition activities of microorganisms, since simple sugar substance is easier to be broken down by it (Cai et al., 2018).

Decomposition of biodegradable pots (filled with soil medium) on the ground

Another experiment included filling of biodegradable pots with soil; decomposition took 60 days on the ground as well. Data in Table 2 show the weight loss percentages in biodegradable pot with ration 50% : 50% – weight loss was significantly higher (51.66%) than in biodegradable pot with ratio B30% : BP70% (46.41%). This finding is contradictory to results presented by Liew and Khor (2015), who reported that higher weight loss occurred in the bioplastic pot made of material with higher cellulose content. This could be attributed to the lower tensile strength of biodegradable pot with lower banana peel content, resulting in the increase of weight loss percentage when the biodegradable pot with ratio B50% : BP50%. was filled with soil. Tensile strength is directly proportional to cellulose content (Ververis et al., 2003). Furthermore, Ullah et al. (2011) also reported that material with higher glycerol concentration biodegraded faster than material with lower glycerol concentration. Authors argued that this was due to the poor strength and bonding between the solid waste and glycerol within the material.

Total carbon (C), nitrogen (N) content and C/N ratio of biodegradable pots

The effect of initial litter quality has been reported to be one of the key drivers of decomposition (Bradford et al., 2016). The C/N ratio of residues is a main factor affecting microbial mineralization of N in crop residues (Vigil and Kissel, 1991; Tian et al., 1992). Increases in C mineralization caused by nitrogen fertilization have been positively related to labile C concentration (Ding et al., 2010). Table 3 shows total content of C, N and C/N ratio of both biodegradable pots. Total content of C in biodegradable pots made of banana peels was higher than total C content in banana peels (Odedina et al., 2017). Total C content in biodegradable pot with ration B50% : BP50% was significantly higher (42.18%) than in biodegradable pot with ratio B30% : BP70% (41.50%). Cellulose polymerization during biomaterial production may have increased the total C content of the biodegradable pots. Since studies (Essien et al., 2005; Kalemelawa et al., 2012) have shown that banana peels are rich in protein and amino acids, the higher N content was expected to be in biodegradable pot with ratio B30% : BP70%. Therefore, biodegradable pot with higher content of banana peels had higher nitrogen content. The C/N ratio of biodegradable pot with ratio B50% : BP50% was significantly higher (137.67) than of biodegradable pot with ratio B30% : BP70% (110.19). It is likely due to higher total N content in biodegradable pot with ratio B30% : BP70%, resulting in the lower C in the biodegradable pot with higher content of banana peels.

Table 2 Weight loss percentages of biodegradable pots with different ratios of biomaterials and banana peels (pots filled with soil medium)

Pots with different ratios of biomaterials (B): banana peels (BP)	Weight loss percentage after 60 days decomposition (%)
B50% : BP50%	51.66^{a} ±0.79
B30% : BP70%	46.41^{b} ±2.29

Different letters in the same column indicate significant differences observed in independent *t*-test at α = 0.05 and ± indicate standard error (n = 3)

Table 3 Total carbon, nitrogen content and C/N ratio of biodegradable pots

Pots with different ratios of biomaterials (B): banana peels (BP)	Total Carbon (%)	Total Nitrogen (%)	C/N Ratio
B50% : BP50%	42.18^{a} ±0.13	0.31^{b} ±0.01	137.67^{a} ±4.40
B30% : BP70%	41.50^{b} ±0.11	0.38^{a} ±0.00	110.19^{b} ±2.23

Different letters in the same column indicate significant differences observed in independent *t*-test at α = 0.05 and ± indicate standard error (n = 3)

A higher C/N ratio found in the biodegradable pot with ratio B50% : BP50% explains a lower weight loss percentage when the empty biodegradable pot B50% : BP50% was left to decompose on the ground.

Conclusions

A higher C/N ratio found in the biodegradable pot with ratio B50%:BP50% explains a lower weight loss percentage after the empty biodegradable pot B50%:BP50% was left to decompose for more than 60 days on the ground. Conversely, weight loss of biodegradable pot with ratio of B50% : BP50% was higher when the pot was filled with soil during 60 days-long decomposition on the ground. It is attributed to lower content of banana peels decreasing the tensile strength of biodegradable pot, making it highly decomposable. Biodegradable pot with ratio B30% : BP70% is better than pot with ratio B50% : BP50% in terms of degradability. Further studies are underway to increase the quality (tensile strength) of biodegradable pot made of banana peels.

Acknowledgement

We express our gratitude to Universiti Malaysia Perlis for providing the facilities to support our research work related to the weight loss of biodegradable pots. This research did not receive any specific grant from funding agencies in the public, commercial, or not-for-profit sectors.

References

BRADFORD, M. A. – BERG, B. – MAYNARD, D. S. – WIEDER, W. R. – WOOD, S. A. 2016. Understanding the dominant controls on litter decomposition. In Journal of Ecology, vol. 104, no. 1, pp. 229–238.

BRIASSOULIS, D. – BABOU, E. – HISKAKIS, M. – SCARASCIA, G. – PICUNO, P. – GUARDE, D. – DEJEAN, C. 2013. Review, mapping and analysis of the agricultural plastic waste generation and consolidation in Europe. In Waste Management Research, vol. 3, no. 12, pp. 1262–1278.

CAI, L. – CHEN, T. B. – ZHENG, S. W. – LIU, H. T. – ZHENG, G. D. 2018. Decomposition of lignocellulose and readily degradable carbohydrates during sewage sludge biodrying, insights of the potential role of microorganisms from a metagenomic analysis. In Chemosphere, vol. 201, pp. 127–136.

DING, W. – YU, H. – CAI, Z. – HAN, F. – XU, Z. 2010. Responses of soil respiration to N fertilization in a loamy soil under maize cultivation. In Geoderma, vol. 155, pp. 381–389.

ESSIEN, J. P. – AKPAN, E. J. – ESSIEN, E. P. 2005. Studies on mould growth and biomass production using waste banana peel. In Bioresource Technology, vol. 96, pp. 1451–1456.

KALEMELAWA, F. – NISHIHARA, E. – ENDO, T. – AHMAD, Z. – YEASMIN, R. – TENYWA, M. M. – YAMAMOTO, S. 2012. An evaluation of aerobic and anaerobic composting of banana peels treated with different inoculums for soil nutrient replenishment. In Bioresource Technology, vol. 126, pp. 375–382.

KAŽIMÍROVÁ, V. – GADUŠ, J. – GIERTL, T. 2018. Verification of suitability of substrate composition for production and quality of biogas. In Acta Technologica Agriculturae, vol. 21, pp. 115–118.

LIEW, K. C. – KHOR, L. K. 2015. Effect of different ratios of bioplastic to newspaper pulp fibres on the weight loss of bioplastic pot. In Journal of King Saud University-Engineering Sciences, vol. 27, pp. 137–141.

ODEDINA, M. J. – CHARNNOK, B. – SARITPONGTEERAKA, K. – CHAIPRAPAT, S. 2017. Effects of size and thermophilic pre-hydrolysis of banana peel during anaerobic digestion, and biomethanation potential of key tropical fruit wastes. In Waste Management, vol. 68, pp. 128–138.

PATIL, P. S. 2015. Behavior of concrete which is partially replaced with waste plastic. In International Journal of Innovative Technology and Exploring Engineering, vol. 4, no. 11, pp. 1–3.

RAMAKRISHNAN, N. – SHARMA, S. – GUPTA, A. – ALASHWAL, B. Y. 2018. Keratin based bioplastic film from chicken feathers and its characterization. In International Journal of Biological Macromolecules, vol. 111, pp. 352–358.

TIAN, G. – KANG, B. T. – BRUSSAARD, L. 1992. Biological effects of plant residues with contrasting chemical compositions under humid tropical conditions-decomposition and nutrient release. In Soil Biology and Biochemistry, vol. 24, pp. 1051–1060.

TOCK, J. Y. – LAI, C. L. – LEE, K. T. – TAN, K. T. – BHATIA, S. 2010. Banana biomass as potential renewable energy resource: A Malaysian case study. In Renewable Energy and Sustainable Energy Reviews, vol. 14, no. 2, pp. 798–805.

ULLAH, A. – VASANTHAN, T. – BRESSLER, D. – ELIAS, A. L. – WU, J. 2011. Bioplastics from feather quill. In Biomacromolecules, vol. 12, no. 10, pp. 3826–3832.

VERVERIS, C. – GEORGHIOU, K. – CHRISTODOULAKIS, N. – SANTAS, P. – SANTAS, R. 2003. Fiber dimensions, lignin and cellulose content of various plant materials and their suitability for paper production. In Industrial Crops and Products, vol. 19, pp. 245–254.

VIGIL, M. F. – KISSEL, D. E. 1991. Equations for estimating the amount of nitrogen mineralized from crop residues. In Soil Science Society of America Journal, vol. 55, pp. 757–761.

VU, H. T. – SCARLETT, C. J. – VUONG, Q. V. 2017. Effects of drying conditions on physicochemical and antioxidant properties of banana (*Musa cavendish*) peels. In Drying technology, vol. 35, no. 9, pp. 1141–1151.

WEBB, H. K. – ARNOTT, J. – CRAWFORD, R. J. – IVANOVA, E. P. 2013. Plastic degradation and its environmental implications with special reference to poly(ethylene terephthalate). In Polymer, vol. 5, pp. 1–18.

DOI: 10.2478/ata-2019-0002

Acta Technologica Agriculturae 1
Nitra, Slovaca Universitas Agriculturae Nitriae, 2019, pp. 5–11

EFFICIENCY COMPARISON OF DIFFERENT PHOTOVOLTAIC MODULES

Atsu Divine KAFUI*, István SERES, István FARKAS
Szent István University, Gödöllő, Hungary

Solar photovoltaic power generation capacity is rising continuously as a result of various regional, sub-regional renewable energy policies and the impact of technology development, as well as the increasing environmental concerns. Characteristics of photovoltaic modules are provided by manufacturers after they have been tested indoors under standard test conditions. These parameters may vary under exterior conditions. It is thus imperative to establish the quantity of the energy produced by photovoltaic modules under real operation conditions. This study sought to assess the performance of different kinds of photovoltaic module technologies in the city of Gödöllő, Hungary, and ascertain the behaviour of the modules under real outdoor conditions. Modules include amorphous silicon (a-Si), monocrystalline silicon (mc-Si), polycrystalline silicon (pc-Si), transparent monocrystalline silicon module (mc-Si). Measurement of the module characteristics was performed and various meteorological parameters were obtained. Performance parameters such as performance ratio and efficiency are given and analysed. Module temperature was estimated and evaluated in comparison with experimental values. Energy conversion rates of the modules were determined as 9.4%, 4.4%, 10.3%, 8.2% and 10.4% for mc-Si module transparent glass (165 Wp), a-Si module (glass 40Wp), pc-Si module (105 Wp), pc-Si module (60 Wp) and mc-Si (PV-T 180 Wp), respectively. Under the given outdoor conditions, the highest average performance ratio of 85.2% was obtained for the mc-Si module (transparent glass, 165 Wp), exhibiting the best performance, while pc–Si module (60 Wp) showed the least average performance ratio of 71.8%.

Keywords: photovoltaic technologies; energy yield; field performance; energy conversion rate

The Sun, a silent, free and non-polluting source of energy, is responsible for all forms of life on earth. Sun's harnessable energy is endless in the nearest foreseeable time, both as a source of heat and light. Without doubt, it is one of the most promising energy source alternatives for meeting the challenges of this millennium. Sunlight, which is available everywhere on the Earth, is virtually responsible for all other energy sources. Therefore, energies from the other energy sources are virtually derived from the Sun.

Solar PV (photovoltaics) has become a ubiquitous source of renewable energy (Bilčík et al., 2018). Solar PV power market is increasing continuously as a result of the various regional, sub-regional and country renewable energy policy schemes. Other factors accounting for this expansion include the depleting status of fossils fuels caused by the increasing energy demand, impact of technology development, lower cost of technology and environmental concerns.

Data sheets of PV modules provide characteristics that are determined by manufacturers in an interior laboratory under a controlled STC (standard test conditions), which include a cell temperature of 25 °C, radiation intensity of 1,000 $W \cdot m^{-2}$ and air mass AM1.5. Not only spectral reactions, temperature coefficients, voltage and current values of individual solar cells and module types differ, but their reactions to environmental factors like radiation, temperature and wind speed vary as well. However, solar spectrum varies depending on geographical location (Atsu et al., 2017).

There is an increase in the diversity of available technologies of solar cells integrated in PV modules – from thin films to crystalline silicon, which still dominates the market with nearly 90% (IEA, 2014). The most common PV module types currently available have energy efficiencies of approximately (7–11)% a-Si and (14–19)% (c-Si, single or double face). Other available module type is triple-junction PV with concentrating lenses with energy efficiency approximately (23–27)%. Future multi-junction cell structures are expected to increase the average efficiency from current 40% to over 50% (King et al., 2012). To choose a particular technology of solar module for an individual site, it is important to establish the energy yield of the module under real meteorological conditions of the specific location.

Studies by Singh (2013), Carr and Pryor (2004), Del Cueto (2002), Cañete et al. (2014) and Balaska et al. (2017) show the dependence of PV energy efficiency and final power output on conditions that deviate from STC for different mounting geometries and PV materials extending the range of useful predictions of PV cells performance.

Majority of these relationships are either theoretical or semi empirical, founded on laboratory measurements, and as a result, they do not incorporate the entire range of interdependencies between the various environmental factors. These, however, may have a pronounce effect on the actual PV efficiency and power output (Durisch et al., 2007).

Contact address: Atsu Divine Kafui, Szent István University, Mechanical Engineering Doctoral School, Páter K. u. 1, H-2100, Gödöllő, Hungary, e-mail: atsud22@yahoo.com

Table 1 Geographical site parameters for Gödöllő (PVsyst 6.7.0)

Period	Global irradiation ($kWh \cdot m^{-2} \cdot d^{-1}$)	Diffuse irradiation ($kWh \cdot m^{-2} \cdot d^{-1}$)	Temperature (°C)	Wind speed ($m \cdot s^{-1}$)
January	0.97	0.69	-0.6	2.78
February	1.84	0.94	1.1	3.00
March	2.93	1.46	5.6	3.41
April	4.41	2.08	11.7	3.10
May	5.53	2.44	17.1	2.99
June	5.99	3.00	19.6	2.89
July	5.98	2.85	21.8	3.09
August	5.00	2.22	21.3	2.71
September	3.60	1.81	15.6	2.61
October	2.31	1.19	11.3	2.6
November	1.14	0.73	5.7	3.00
December	0.81	0.51	0.2	2.49
Year average	**3.38**	**1.66**	**10.9**	**2.49**

Considering this area, multiple studies have been conducted in different locations to assess the impact of environmental factors on the performance of different cell technologies or numerous studies have set their goals to determine the best operation conditions for the specific sites.

Study by Ye et al. (2014) evaluates the performance of a-Si and mc-Si modules according to radiation distribution, temperature and other external environment factors – authors observed that a-Si modules were more efficient in the blue rich spectrum, whereas the mc-Si modules showed efficiency varying with changes in cell temperature. Sharma et al. (2013) evaluated different on-grid PV systems with arrays of different module technologies in India. They concluded that systems with a-Si and HIT modules showed better results than pc-Si modules.

Cañete et al. (2014) performed a comparative study under meteorological conditions in Southern Spain on four different PV module technologies: a-Si, tandem structure of a-Si/μc-Si, cadmium telluride (CdTe) and pc-Si module. Results of their study showed that performance of thin film modules is better than that of pc-Si modules for this location.

Basoglu et al. (2015) compared the energy performance of three different PV module technologies under Izmit, Kocaeli climatic conditions in Turkey. Module technologies were mc-Si, c-Si and CdTe. They concluded that CdTe modules are more acceptable for climatic condition in Izmit.

Aforementioned studies have shown that each of the PV technologies has unique merits and limitations in operation under various climatic conditions (Cristina et al., 2014).

The amount of usable solar radiation at any site is dependent on the angle of inclination and equipment orientation, as well as on intensity of total solar radiation. In comparison to other European countries, Hungary has more favourable conditions for PV. Annual sunshine hours range between 1,900 and 2,200 hours. Annual average global irradiation of Gödöllő is approximately 3.38 $kWh \cdot m^{-2} \cdot d^{-1}$ and diffuse irradiation is 1.66 $kWh \cdot m^{-2} \cdot d^{-1}$ (Table 1). This makes Hungary an appropriate location for the utilization of solar energy for energy generation.

Our study aims to assess the performance of different kinds of PV module technologies (a-Si, mc-Si, pc-Si, transparent mc-Si) under real outdoor conditions. Performance parameters, such as performance ratio and efficiency, are given and analysed.

Material and methods

Experimental setup

Experimental setup was located at the Solar Energy Laboratory of the Szent István University, Gödöllő, Hungary situated at latitude 47° 35′ 39″ N, longitude 19° 22′ 0″ E. PV modules types used and their specifications under laboratory STC are summarized in Table 2. PV modules were inclined to a fixed physical support outside the lab and oriented to the south with an inclination corresponding to the site latitude. The modules' output power, voltage and current were measured automatically using the Geräte Unterricht Naturwissenschaft Technik (G.U.N.T) PV setup as shown in Fig. 1. Solar radiation was measured with a Kimo solarimeter LSL 200 at the level and inclination of the PV modules (resolution 1 $W \cdot m^{-2}$, accuracy 5%). Temperature of PV modules, ambient temperature of PV modules and ambient temperature were measured using HT-9815 Xintest Pt-100 sensors (±0.1 °C).

Performance analysis

Performance of individual modules was evaluated in accordance the IEC standard (IEC 61724) describing the parameters of solar modules. Certain parameters like yield, performance ratio efficiency, were calculated.

Module yield

Specific module yield (Y_a) is defined as the ratio of the energy output from the module to a particular duration to its rated power:

Fig. 1 PV modules and experimental setup for data collection

Table 2 Technical specifications of PV modules under STC

Parameters	a-Si (Glass) (DUNA SOLAR)	mc-Si (Glass) (SOLARWATT)	pc-Si (60Wp) (SOLAREX SM2160)	pc-Si (105Wp) (RWE SCHOTT SOLAR)	PV-T glazed (mc-Si) (SOLIMPEKS)
V_{oc} (V)	62.5	23.4	21.3	29.5	43.39
I_{sc} (A)	1.15	9.02	3.8	4.92	5.55
V_{mpp} (V)	44.0	19.2	17.1	23.5	35.15
I_{mpp} (A)	0.90	8.71	3.5	4.47	5.12
P_{mpp} (Wp)	40	165	60	105	180
Module area (m^2)	0.791	1.62	0.564	0.826	1.427
Temp. coeff. of power	-0.47	-0.40%/°C	-0.47	-0.47%/°C	-0.45%/°C
Temp. coeff. of V_{oc}	-0.36%/	-0.32%/°C	-0.073%/°C	-0.38%/°C	-0.34%/°C
Temp. coeff. of I_{sc}	+0.04%/	0.05%/°C	0.003%/°C	+0.10%/°C	+0.06%/°C
Efficiency	5%	10.3%	10.6%	12.7%	12.6%

PV-T – photovoltaic thermal, V_o – open circuit voltage, I_{sc} – short circuit current

$$Y_a = \frac{E_{DC}}{P_{PV_{rated}}} \tag{1}$$

Solar module temperature

Considering the calculation of the module temperature (T_c), following model is used:

$$T_c = T_a + \frac{G}{G_{STC}} \times (T_{NOCT} - 20) \tag{2}$$

where:

T_a – ambient temperature (°C)
T_{NOCT} – nominal operating cell temperature given by the manufacturer (°C) (NOCT – nominal operating cell temperature)
G – measured solar irradiation over the surface of the module (W·m^{-2}) (Duffie and Beckman, 2006)

Solar module output power

Solar module output power is calculated from the model taking into account the linear dependence of output power on the solar irradiance and cell temperature. It is given by Eq. (3):

$$P_m = P_{mSTC} \times \frac{G}{G_{STC}} \times \left(1 - \gamma(T_C - 25)\right) \tag{3}$$

where:

P_m – calculated output power (W)
$P_{m.STC}$ – maximum rated power at STC given by the manufacturer (W)
G – solar radiation intensity on the plane of the module (W·m^{-2})
G_{STC} – solar radiation intensity of 1,000 W·m^{-2}
γ – maximum power correction factor for temperature
T_c – module temperature (°C)

Solar module efficiency

Instantaneous efficiency of the module is defined as follows:

$$\eta = \frac{P}{(G \times A)} \tag{4}$$

where:

η – efficiency (%)
P – measured power output (W)
G – measured solar irradiation (W·m^{-2})
A – suarface area of the module (m^2) (Duffie and Beckman, 2006)

However, model given by Eq. (5) is necessary for calculation of instantaneous efficiency:

$$\eta = \eta_{Tref}\left(1 - \beta_{ref}(T_c - T_{ref}) + \gamma \lg G_T\right) \quad (5)$$

where:

- η – instantaneuos efficiency;
- η_{Tref} – efficiency at the reference condition (%)
- β_{ref} – temperature coefficient
- T_{ref} – temperature at the reference condition (°C)
- T_c – solar module temperature (°C)
- γ – correction factor for the irradiance
- G_T – solar irradiance intensity (W·m^{-2}) (Almonacid et al., 2011)

However, following module is used for the majority of c-Si modules:

$$\eta = \eta_{Tref}\left(1 - \beta_{ref}(T_c - T_{ref})\right) \quad (6)$$

where:

- η – instantaneuos efficiency
- η_{Tref} – efficiency at the reference condition (%)
- T_{ref} – temperature at the reference condition (°C)
- β_{ref} – temperature coefficient
- T_c – solar module temperature (°C)

Performance ratio (PR)

Performance ratio is the ratio of the PV module/system efficiency during operation to its efficiency at STC as given by Eq. (7):

$$PR = \frac{\eta_{syst}}{\eta_{STC}} \quad (7)$$

PR shows the closeness of a PV system to the ideal performance during real operation conditions and allows comparison of PV systems independently of location, tilt angle, orientation and their nominal rated power capacity (Ayompe et al., 2011).

Results and discussion

This part explains the measured data obtained during the experiment in detail and compares measured data for the individual modules with the characteristics given by manufacturer.

Incident radiation onto the modules was quite stable throughout the period of the experiment. Maximum value observed was 965 W·m^{-2} and minimum value recorded was 915 W·m^{-2} with an average radiation of 935 W·m^{-2} as shown in Fig. 2. Ambient temperature and module temperature measured are shown in Fig. 3. Results indicate a maximum ambient temperature of 37 °C and an average temperature of 35 °C for the experiment duration.

The pc-Si (105Wp) module had the highest recorded temperature (61 °C) during the experiment. Minimum temperature of 54.7 °C was observed in the mc-Si (165Wp) glass module. Average temperatures of the various modules were 57.7 °C, 58.9 °C, 58.7 °C, and 58.0 °C for mc-Si 165Wp

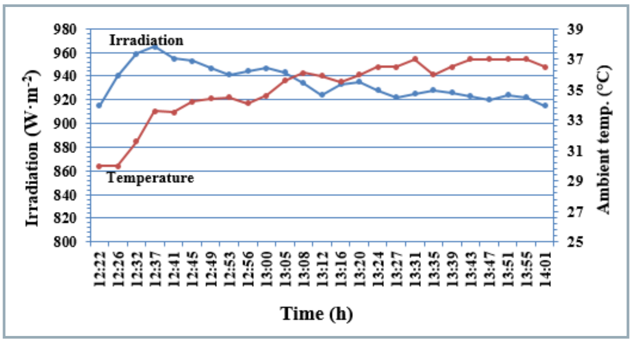

Fig. 2 Variation in ambient temperature with irradiation

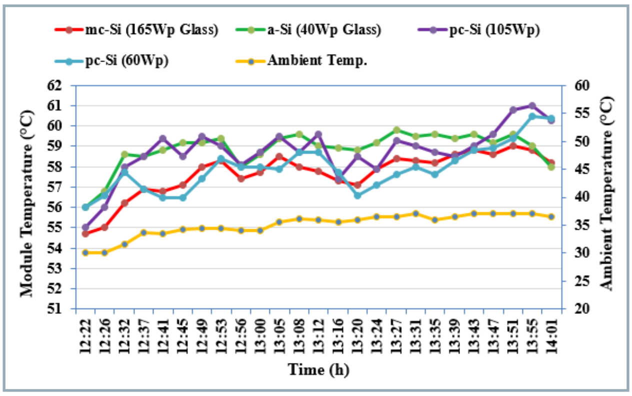

Fig. 3 Trends in module and ambient temperatures

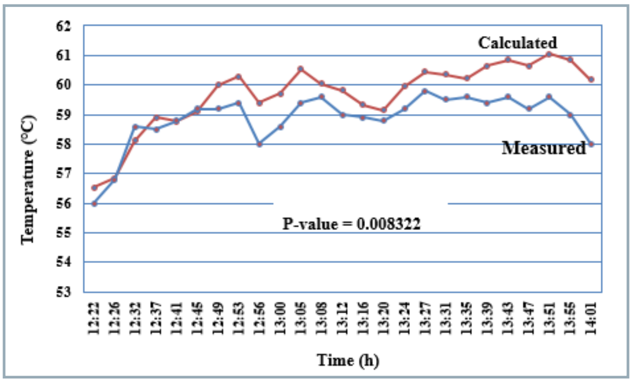

Fig. 4 Comparison between calculated and measured module temp. a-Si (40 Wp Glass)

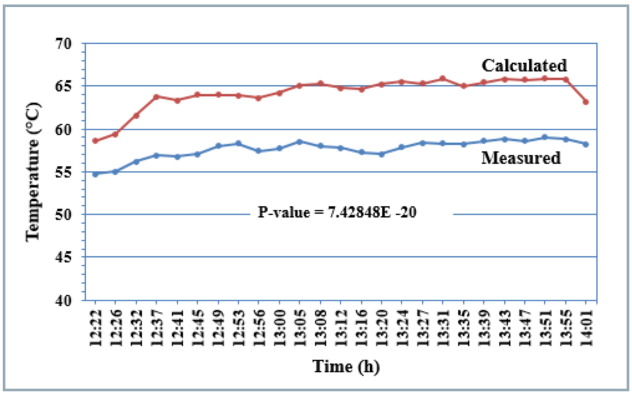

Fig. 5 Comparison between calculated and measured module temp. (mc-Si -165 Wp Glass)

glass, a-Si 40Wp Glass, pc-Si, 105Wp, pc-Si 60Wp respectively. Maximum average value of 58.87 °C was observed in the a-Si 40Wp glass module and minimum average temperature of 57.77 °C was observed in mc-Si 165 Wp glass module.

As Figs. 4, 5, 6, and 7 show, calculated average module temperature was 58.76 °C. Subsequently, minimum and maximum values were 55.64 °C and 60.16 °C respectively.

Measured temperatures for mc-Si (165 Wp Glass) were lower than the calculated module temperatures throughout the entire experiment as shown in Fig. 5. Mc-Si (165 Wp Glass) also showed the highest significant deviation between the measured and calculated values. With the exception of the pc-Si (105 Wp), which showed no significant difference between the measured and calculated temperatures, the mc-Si (165 Wp glass), a-Si (40 Wp) and pc-Si (60 Wp) had significant deviations as shown by their *P*-values. The greatest deviation was observed in the mc-Si -165 Wp module.

Measured average temperatures for the modules were 57.66; 58.87; 58.74 and 57.93 °C for mc-Si (165 Wp glass), a-Si (40 Wp), pc-Si (105 Wp) and pc-Si (60 Wp) respectively. Each module showed a different trend of measured temperatures corresponding with the calculated module temperatures as shown in Figs. 4, 5, 6, and 7.

Fig. 8 demonstrates the module efficiencies with variation in irradiation levels – initial high efficiency values of all modules are as a result of increasing irradiation (for initial 20 minutes). Subsequently, after this point, there is a gradual decrease in irradiation with corresponding decrease in efficiency for all the modules.

Figs. 9, 10, 11 and 12 present the relationships between the efficiencies and module temperatures. Results show a corresponding decrease in efficiency for all studied modules with increases in the module temperatures.

However, this trend of efficiency decreasing is not smoothly continuous. Corresponding effect of change in temperature of the module, whether increasing or decreasing, can be seen in the varying efficiency of the modules. However, for the pc-Si (105 Wp) module, the efficiency of the module began to increase with increase in module temperature at module temperature ≥58 °C.

Table 3 compares the efficiencies determined by experimental data with manufacturer's values.

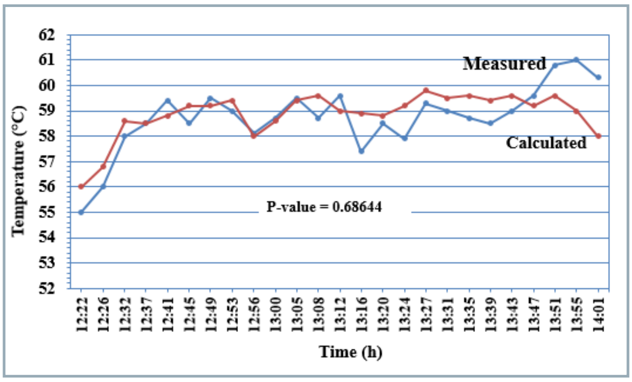

Fig. 7 Comparison between calculated and measured module temp. pc-Si (105Wp)

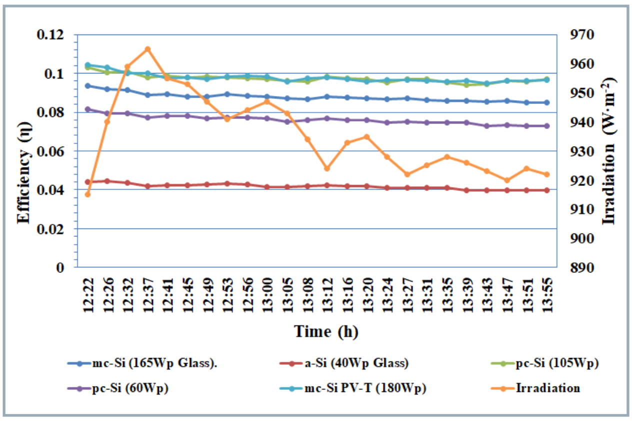

Fig. 8 Variation of efficiency of modules with irradiation

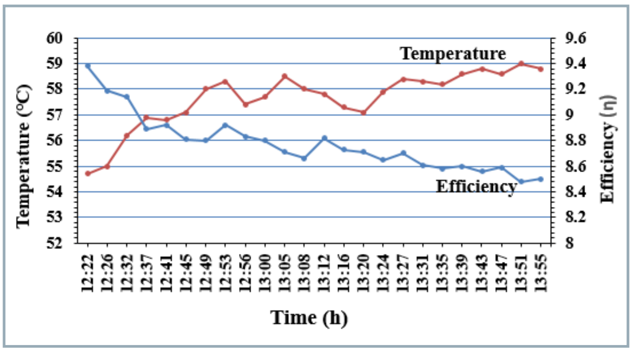

Fig. 9 Relationship between efficiency and temperature of module mc-Si (165 Wp Glass)

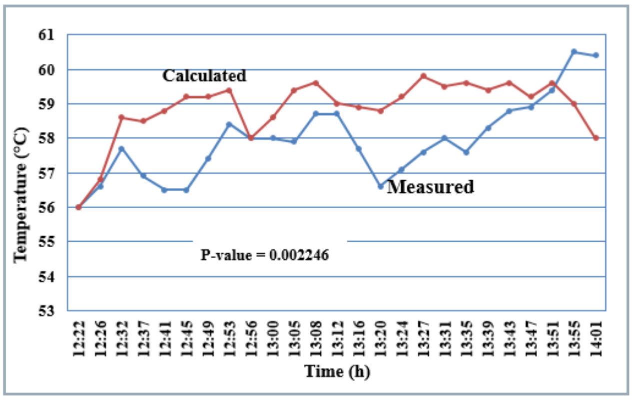

Fig. 6 Comparison between calculated and measured module temp. pc-Si (60Wp)

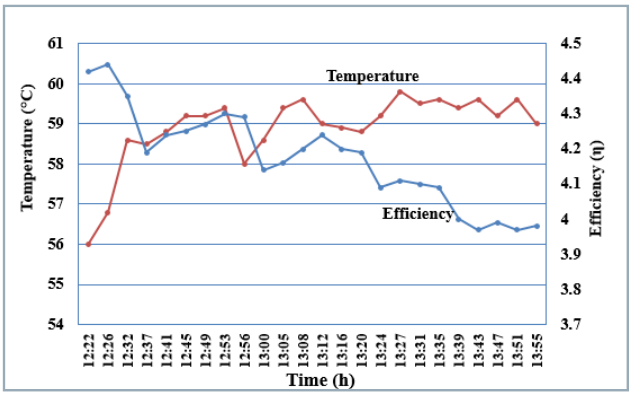

Fig. 10 Relationship between efficiency and temperature of module a-Si (40Wp Glass)

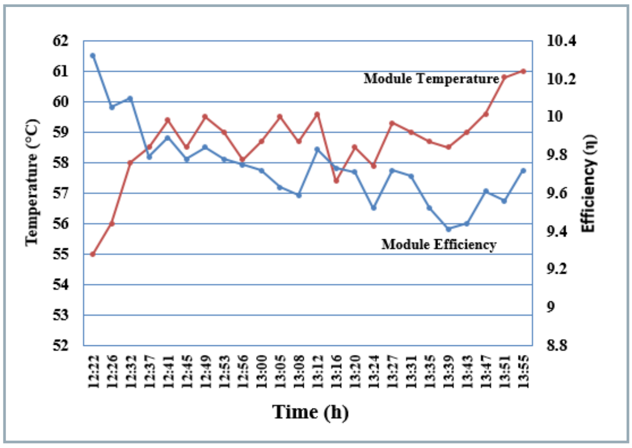

Fig. 11 Relationship between efficiency and temperature of module pc-Si (105 Wp)

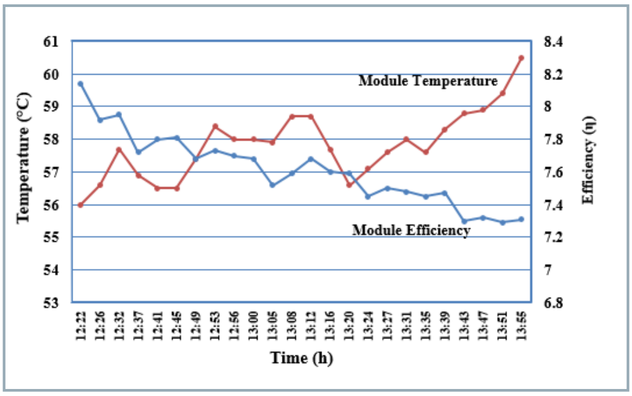

Fig. 12 Relationship between efficiency and temperature of module pc-Si (60 Wp)

Results show varying deviations depending on the technology. As shown in Table 3, the highest deviation from the manufacturer's values was 2.4, obtained for pc-Si module (60 Wp), while the lowest deviation from the given manufacturer's efficiencies was 0.6, obtained for a-Si module (40 Wp). It is worth mentioning that this module has already been in operation for approximately 20 years. However, the highest percentage deviation of -22.6% was recorded for the pc-Si module (60 Wp), while the minimum percentage deviation of -8.7% was obtained for the mc-165 Wp transparent module as shown in Table 3. In literature, results by Balaska et al. (2017) indicated daily mean efficiencies of 8.38% and 12.63% for m-Si_μc-Si, and mc-Si, respectively. Cañete et al. (2014) also recorded an efficiency of 9.3% for CdTe, 6.3% for a-Si, 13.2% for pc-Si and 8.0% for a-Si/μmc-Si. Determining the percentage deviation between the manufacturer's values and the experimentally obtained efficiency, Cañete et al. (2014) recorded -4.1% deviation for CdTe, -4.8% for a-Si, -5.9% for a-Si/μmc-Si and -1.5% for pc-Si.

The performance ratios for the modules are presented in Table 4. The mc-Si transparent glass module (165 Wp) showed the highest average performance ratio PR of 85.2%. The lowest average PR of 71.8% was obtained for pc-Si module (60 Wp).

Average PR of 82.6%, 77.5%, and 76.7% were recorded for a-Si module (glass 40 Wp), PV-T (180 Wp) and pc-Si module (105 Wp), respectively. Cañete et al. (2014), however, observed an annual average PR of 94.8% for a-Si, 92.9% for pc-Si, and 93.9% for a-Si/μmc-Si.

Conclusions

Performance analyses were carried out for five different modules under the same outdoor conditions. Modules were exposed to an average irradiation of 935 W·m^{-2} and average ambient temperature of 35 °C. Energy conversion rates of the modules were determined as 9.4%, 4.4%, 10.3%, 8.2% and 10.4% for mc-Si glass module (165Wp), a-Si glass module (40Wp), pc-Si module (105 Wp), pc-Si module (60 Wp) and PV-T (180 Wp) respectively. Under the given outdoor conditions, the highest average PR of 85.2% was obtained for the mc-Si glass module (165Wp) exhibiting the best performance; the lowest average PR of 71.8 was observed in case of pc-Si module (60 Wp).

Table 3 Comparison between experimental and manufacturer's module efficiency

Module technology	mc-Si module glass (165 Wp)	a-Si module glass (40 Wp)	pc-Si module (105Wp)	pc-Si module (60Wp)	PV-T glazed mc-Si (180 Wp)
Datasheet efficiency (DE) (%)	10.3	5	12.7	10.6	12.6
Measured efficiency (ME) (%)	9.4	4.4	10.3	8.2	10.4
(DE-ME)/DE	-8.7%	-12%	-18.9%	$^{-2}$2.6%	-17.5%

Table 4 Performance ratios (PR) of modules

Performance ratios (PR) of modules	mc-Si (glass) (165 Wp)	a-Si (glass) (40 Wp)	pc-Si (105 Wp)	pc-Si (60 Wp)	PV-T glazed mc-Si (180 Wp)
Minimum	0.83	0.79	0.74	0.69	0.75
Maximum	0.91	0.89	0.81	0.77	0.83
Average	85.2%	82.6%	76.7%	71.8%	77.5%

Acknowledgement

This work was supported by the Stipendium Hungaricum Programme and the Mechanical Engineering Doctoral School, Szent István University, Gödöllő, Hungary.

References

ALMONACID, F. – RUS, C. – PEREZ-HIGUERAS, P. – HONTONA, L. 2011. Calculation of the energy provided by a PV generator. Comparative study: conventional methods vs artificial neutral network. In Energy, vol. 36, pp. 375–384.

ATSU, D. – SERES, I. – FARKAS, I. 2017. Performance evaluation of solar photovoltaic modules under real conditions. In Book of Abstracts, 23th Workshop on Energy and Environment, Gödöllő, Hungary, November 30-December 1, 2017, p. 20.

AYOMPE, L. M. – DUFFY, A. – MCCORMACK, S. J. – CONLON, M. 2011. Measured performance of a 1.72 kW rooftop grid connected photovoltaic system in Ireland. In Energy Conversion and Management, vol. 52, no. 2, pp. 816–825.

BALASKA, A. – TAHRI, A. – TAHRI, F. – STAMBOULI, A. B. 2017. Performance assessment of five different module technologies under outdoor conditions in Algeria. In Renewable Energy, vol. 107, pp. 53–60.

BASOGLU, M. E. – KAZDALOGLU, A. – ERFIDAN, T. – BILGIN, M. Z. – CAKIR, B. 2015. Performance analysis of different photovoltaic module technologies under Izmit, Kocaeli climate conditions. In Renewable and Sustainable Energy Reviews, vol. 52, pp. 357–365.

BILČÍK, M. – BOŽIKOVÁ, M. – PETROVIČ, A. – MALÍNEK, M. – CVIKLOVIČ, V. – OLEJÁR, M. – ARDONOVÁ, V. 2018. Analysis of selected photovoltaic panels operating parameters as a function of partial shading and intensity of reflected radiation. In Acta Technologica Agriculturae, vol. 21, no. 1, pp. 14–17.

CAÑETE, C. – CARRETERO, J. – SIDRACH-DE-CARDONA, M. 2014. Energy performance of different photovoltaic module technologies under outdoor conditions. In Energy, vol. 65, pp. 295–302.

CARR, A. J. – PRYOR, T. 2004. A comparison of the performance of different PV module types in temperate climates. In Solar Energy, vol. 76, pp. 285–294.

CRISTINA, C. – JESUS, C. – MARIANO, S. 2014. Energy performance of different photovoltaic module technologies under outdoor conditions. In Energy, vol. 65, pp. 295–302.

DEL CUETO, J. 2002. Comparison of energy production and performance from flat plate photovoltaic module technologies deployed at fixed tilt. In Proceedings of the 29th IEEE photovoltaic specialists conference (2002), pp. 1523–1526.

DUFFIE, J. A. – BECKMAN, W. A. 2006. Solar Engineering of Thermal Processes. New York, Wiley. 928 pp. ISBN 0-471-69867-9.

DURISCH, W. – BITNAR, B. J. – MAYOR, H. – KIESS, K. – LAM, J. 2007. Efficiency model for photovoltaic modules and demonstration of its application to energy yield estimation. In Solar Energy Materials and Solar Cells, vol. 91, pp. 79–84.

INTERNATIONAL ENERGY AGENCY (IEA). 2014. Technology Roadmap. Solar Photovoltaic Energy.

KING, R. R. – BHUSARI, D. – LARRABEE, D. – LIU, X. Q. – REHDER, E. – EDMONDSON, K. – COTAL, H. – JONES, R. K. – ERMER, J. H. – FETZER, C. M. – LAW, D. C. – KARAM, N. H. 2012. Solar cell generations over 40% efficiency. In Progress in Photovoltaics: Research and Applications, vol. 20, pp. 801–815.

SHARMA, V. – KUMAR, A. – SASTRY, O. – CHANDEL, S. 2013. Performance assessment of different solar photovoltaic technologies under similar outdoor conditions. In Energy, vol. 58, pp. 511–518.

SINGH, G. 2013. Solar power generation by PV (photovoltaic) technology: a review. In Energy, vol. 53, pp. 1–13.

YE, J. Y. – REINDL, T. – ABERLE, A. G. – WALSH, T. M. 2014. Performance degradation of various PV module technologies in tropical Singapore. In IEEE Journal of Photovoltaics, vol. 4, pp. 1288–1294.

DOI: 10.2478/ata-2019-0003

Acta Technologica Agriculturae 1
Nitra, Slovaca Universitas Agriculturae Nitriae, 2019, pp. 12–16

CHOOSING A PROPER MAINTENANCE AND REPAIR STRATEGY FOR TRACTORS (IN URMIA)

Razieh POURDARBANI

University of Mohaghegh Ardabili, Ardabil, Iran

Maintenance plays an important role in reliability, availability, production quality, risk reduction, efficiency increasing, equipment security, etc. Therefore, maintenance strategies have a special position in industry. Simultaneously, effect of tractor power is considerable in agriculture; therefore, it is necessary to pay attention to the probability of failure, repair time and causes of malfunctioning. Many variables, including cost, depreciation, breakdowns, annual performance, etc., have major impact on tselection of a maintenance strategy. Therefore, these variables were determined with the help of experts. Subsequently, these were clustered into several main criteria groups on the basis of factor analysis using SPSS software. Obtained results were used in a hierarchical structure to suggest the most appropriate maintenance strategy based on pair-wise comparison. According to the regional conditions and available facilities, results showed that the proactive maintenance strategy proved to be the best suggested option from four maintain strategies, namely emergency maintenance, proactive maintenance, preventive maintenance, predictive maintenance.

Keywords: maintenance strategy; factor analysis; analytical hierarchical process

As agricultural industry is rapidly expanding and it will have to compete with large companies in near future, managers should be prepared to adapt to new management systems, including maintenance management in order to achieve the best efficiency and reliability. In fact, prediction of the exact time of failures and their repairs can lead to a reduction in the cost of repairs and time delays in the machinery operation, more efficient planning, higher safety, increase in financial savings and higher economic returns (Khodabakhshian et al., 2008). In Iran, repairs and replacement costs show a relatively high figure in terms of global standards. In order to automate the production in the agricultural sector, reducing these costs can significantly help to the proper operation of machines and eliminate the disadvantages (Jafari and Mahvi Diani, 2003). Maintenance is usually referred to as all activities that must be performed to ensure the reliability and operation of a device and minimize the number of sudden failures (Bartholomew, 1981; Zasadzień and Midor, 2018). This approach has gradually been introduced into the industry since the 1970s (Dahunsi, 2008).

Maintenance methods that have been invented over the past years include: (a) non-programmed system, in which the repairs take place after the system is stopped and emergency repairs are necessary, and (b) programmed systems, in which an earlier schedule for maintenance and repair activities is developed. Main purpose of these systems is to prevent emergency repairs and unexpected stops. It includes sub-systems, namely proactive maintenance (PAM), preventive maintenance (PM) and predictive maintenance (PDM). Preventive maintenance (PM) focuses its policy on pre-failure repairs, and is particularly suited to industries with high sensitivity to process changes and unplanned changes to the system. It provides appropriate instructions for periodic maintenance or replacement of parts particularly in the case of continuous and mass production systems (Shirmohammadi, 2002). Predictive maintenance (PDM) is a graphical process for detecting, analysing and repairing equipment problems before failure. In fact, existence of weaknesses as such increases preventive maintenance activity and prompts the users to check instantaneously the condition of the equipment from the point of view of temperature, pressure, and other factors by installing measuring equipment and with the help of the software. Installation of such systems is expensive and frequently comes with complex equipment and it is questionable whether the degree of process sensitivity can justify the utilization of such systems. Proactive maintenance (PAM) prevents the source of failure from developing by modifying the conditions that could lead to the destruction of the system. In such manner, it can ensure high reliability, pro-long the life of mechanical equipment and avoid critical failures.

Behzad et al. (2007) performed measurements of vibrations at appropriate locations and evaluated the process of these vibrations and their frequency spectra at water pumping stations with a predictive maintenance approach. Taking into account that obtained frequency spectra were indicative of defect type, defects were detected before the critical state occurred and repairs were performed. Mirzakhani (2004) conducted a study on

Contact address: Razieh Pourdarbani, University of Mohaghegh Ardabili, Department of Biosystem Engineering, Ardabil, Iran, e-mail: r_pourdarbani@uma.ac.ir

vibration analysis as a foundation for proactive maintenance in cement company. As time went by, it was noted that average vibrations of devices were reduced. However, these vibrations sometimes increased due to no particular reason. After performing the necessary repairs and adjustments, vibration parameters were reduced again. Afsharnia et al. (2013) studied the effect of maintenance policies on failure rate of various systems in the Messier Ferguson 399 tractor in Khuzestan by means of a questionnaire and direct interviews in five province zones. Regression analysis, carried out using the exponential function estimation, revealed that different tractors, which were repaired in the past, showed significant signs of wear. Tractors subjected to preventive maintenance, however, also showed severe wear – their engine and steering were past their service life; hydraulic system and cooling were at the end of their service life and at the brink of burnout phase; power system and power transmission system were in phase of initial failures; brake and fuel systems were at the end of the life cycle, which would quite likely develop to the burnout phase. Say and Sumer (2011) conducted a study on the analysis of the linear degradation rate of compound planter and came to conclusion that breakdowns were largely influenced by annual operating hours, maintenance policies and work environment. Mousavi Pour et al. (2012) examined the condition of sugar cane harvesting machines and methods for their maintenance and repair, emphasizing oil status monitoring method. Results showed that use of oil status monitoring method resulted in reduction of malfunctions by 22% in standby machines and by 13% in refurbished machines in comparison to emergency maintenance strategy. Exner et al. (2017) conducted a research on proactive maintenance as success factor for use-oriented Product-Service Systems. In use-oriented Product-Service Systems (PSS), ownership of the product remains with the provider who is responsible for maintenance, repair and overhaul. Therefore, risk of machine unavailability is transferred from the customer to the PSS provider. In order to minimize this risk, the provider needs to reduce unscheduled downtimes to enhance machine availability. Hence, proactive maintenance is an important success factor for providing this PSS type.

Currently, Urmia's maintenance system is based on an emergency strategy. Selection of this strategy in the past was due to the lack of familiarity with the premature costs of operations caused by stagnation and stopping of the machine. However, adequate maintenance policy is vital for the mass production and reduction of stops in production is essential for it. However, one of the primary questions in managing and adopting to a new management system is to decide and select the appropriate option from the existing strategies. We tried to select appropriate strategy for the existing facilities and capital in this paper.

Material and methods

This research was conducted in Urmia in 2016. In order to select the most adequate maintenance strategy for the mechanization service companies, firstly, it is necessary to identify the factors affecting the maintenance techniques. These factors were determined by experts, including representatives from technical departments, repair shops, dealers and service companies. Due to the large number of criteria, it was necessary to select a statistical method for summarizing the data, which would convert the criteria to sub criteria called factors, with help of factor analysis in SPSS Statistics 23. First of all, it selects a combination of variables, correlations of which show the highest amount of variance observed; this sets factor 1. Factor 2 is a set of variables that has the highest contribution in explaining the remaining variance. This method is also applied for the third, fourth, and subsequent factors, so that all variables can be clustered (Fig. 1).

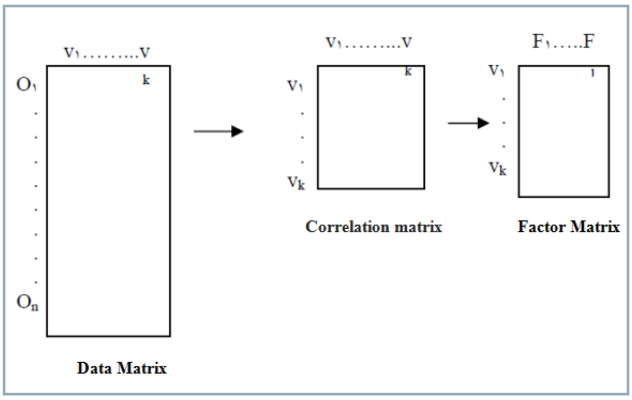

Fig. 1 Data transfer to clusters

If Y_i is the observed variable and $F1$ and $F2$ are two effective factors, mathematical expression of the factor analysis can be written as follows (Richards, 1983):

$$Y_i = \lambda_{i1}F_1 + \lambda_{i2}F_2 + (1)e_i \tag{1}$$

$$\mathrm{Var}(Y_i) = \lambda_{i1}^2\mathrm{Var}(F_1) + \lambda_{i2}^2\mathrm{Var}(F_2) + (1)^2\,\mathrm{Var}(e_i) = \lambda_{i1}^{\ 2} + \lambda_{i2}^2 + \partial_i^2$$

$$\mathrm{Var}(Y_i) = \lambda_{i1}^2 + \lambda_{i2}^2 + \partial_i^2$$

If there are n variables and m factors, the matrix expression of the subject is as follows:

$$\begin{aligned} X_1 &= \lambda_{11}F_1 + \lambda_{12}F_2 + \ldots + \lambda_{1m}F_m + e_1 \\ X_2 &= \lambda_{21}F_1 + \lambda_{22}F_2 + \ldots + \lambda_{2m}F_m + e_2 \\ &\ldots \\ X_n &= \lambda_{n1}F_1 + \lambda_{n2}F_2 + \ldots + \lambda_{nm}F_m + e_n \end{aligned} \tag{2}$$

$$\begin{bmatrix} X_1 \\ \vdots \\ \vdots \\ X_n \end{bmatrix}_{n\times1} = \begin{bmatrix} \lambda_{11} & \cdots & \cdots & \lambda_{1m} \\ \vdots & \ddots & & \vdots \\ \vdots & & \ddots & \vdots \\ \lambda_{n1} & \cdots & \cdots & \lambda_{nm} \end{bmatrix}_{n\times m} \begin{bmatrix} F_1 \\ \vdots \\ F_m \end{bmatrix}_{m\times1} + \begin{bmatrix} e_1 \\ \vdots \\ \vdots \\ e_n \end{bmatrix}_{n\times1} \tag{3}$$

$$X_{n\times1} = A_{n\times m}F_{m\times1} + e_{n\times1}$$

If the factors fully describe the observed variables, then it is possible to write:

$$e_1 = e_2 = e_3 = 0 \Rightarrow \sigma_1^2 = \sigma_2^2 = \sigma_3^2 = 0 \tag{4}$$

$$X_{n\times1} = A_{n\times m}F_{m\times1}$$

After determining the factors, it is necessary to design the Analytical Hierarchical Process (AHP) and make comparisons between the various decision options. Therefore, a set of matrices, which numerically measures the relative importance of the indices relative to each other and each decision option, is measured according to the indices relative to the other options. This is carried out by making paired comparison between the decision elements. To do this, the *i*-th indices are often compared to the *j*-th indices (Table 1).

Table 1 Pairwise comparison scale

Judgment	Value
Extremely important	9
	8
Very strongly more important	7
	6
Strongly more important	5
	4
Moderately more important	3
	2
Equally important	1

Initially, the weight of factors derived from factor analysis was calculated by means of pair comparison matrix and the integration of expert group views through the geometric mean (Table 3). An incompatibility rate of less than 0.1 represents a good match, otherwise, it should be re-evaluated in comparisons. Subsequently, coefficient of priority of each factor was obtained in four criteria of proactive, preventive, predictive and emergency maintenance strategy by the paired matrix in the Expert Choice software (Table 3). Weight of the factors is then calculated in accordance with Table 4. At this stage, in order to rank the decision matrix criteria, we must multiply the weight of each factor by the weight of the options until its final weight is obtained. Final weight of each option that has the highest value is selected as appropriate option.

Results and discussion

By entering the criteria related to maintenance strategy, the following results were obtained in the SPSS software and the factor analysis.

Figures showed in the table above represent the specific values, and the higher the absolute value of a particular parameter value in a factor, the greater the allocation of this parameter to that particular factor. In some cases, however, values are close to several factors, and assigning the parameter to a particular factor causes some data to be lost. For example, there are hesitations whether to allocate the wage repair parameter to factors 2 and 3. Therefore, for better interpretation, as well as better determination of number of factors, the invariant invariance with the Vari-max criterion is used to simplify the inverse matrix columns. Results are presented in Table 5. After rotation of factors, allocation of parameters to the factors is more accurate and shows lower amount of errors. By the

Table 2 Matrix of pair-wise comparison of factors

	Factor 1	Factor 2	Factor 3	…	Factor *n*	Eigenvector
Factor 1	f11	f12	f13	…	f13	v1
Factor 2	f21	f22	f23	……	f23	v2
…….	……	……	……	……	……	……
Factor *n*	f*n*1	f*n*2	f*n*3	……	f*n*3	v*n*

Table 3 Matrix of pair-wise comparison of criterion for each factor

Factor *n*	Criterion 1	Criterion 2	……	Criterion *m*	Eigenvector
Criterion 1	A11	A12	……	A*m*1	Vc*n*1
Criterion 2	A21	A22	……	A*m*1	Vc*n*2
….	…..	…..	……	……..	……
Criterion *m*	A*m*1	A*m*2	……	A*mm*	Vc *nm*

Table 4 Matrix of pair-wise comparison of weight of each factor on the basis of criteria

	Factor 1	Factor 2	…….	Factor *n*
Criterion 1	V11	V12	……	*V*1*n*
Criterion 2	V21	V22	……	*V*2*n*
….	……	……	……	……
Criterion *m*	*Vm*1	*Vm*2	……	*Vmn*

Table 5 Factor analysis results before and after inversion rotation

	Before rotation of factors			After rotation of factors		
Parameter	**Factor 1**	**Factor 2**	**Factor 3**	**Factor 1**	**Factor 2**	**Factor 3**
Fuel cost	0.956	-0.233	-0.147	0.954	0.247	-0.147
Lubrication cost	0.949	-0.248	-0.155	0.952	0.237	-0.157
Cost of spare parts	0.529	0.744	-0.199	0.189	0.876	0.259
Wage repair	0.414	**0.633**	**-0.652**	0.077	0.974	-0.206
Reliability	0.864	-0.381	-0.251	-0.679	-0.497	-0.496
Annual Function	0.99	-0.023	-0.033	0.918	0.368	0.065
Depreciation	0.991	-0.093	-0.071	0.941	0.333	-0.003
Equipment	0.956	-0.233	-0.147	0.954	0.247	-0.141
Stagnation	0.856	-0.345	0.321	0.951	-0.109	0.197
Period of repair	0.438	0.708	0.545	0.194	0.449	0.867
Number of failures	0.736	-0.502	0.446	0.912	-0.34	0.214
Training	0.81	0.313	0.155	0.644	0.472	0.374
Education	0.313-	0.272	0.902	-0.298	-0.35	0.88

Table 6 Classification of factors

Factor 1	– fuel cost, lubrication cost, reliability, annual function, depreciation, equipment, stagnation, number of failures, training
Factor 2	– cost of spare parts, wage repair
Factor 3	– education, period of repair

Table 7 Weight of factors in maintenance strategies

Criteria	**Factor 1**	**Factor 2**	**Factor 3**
EM	0.053	0.658	0.055
PM	0.316	0.155	0.125
PdM	0.316	0.11	0.175
PAM	0.316	0.078	0.644

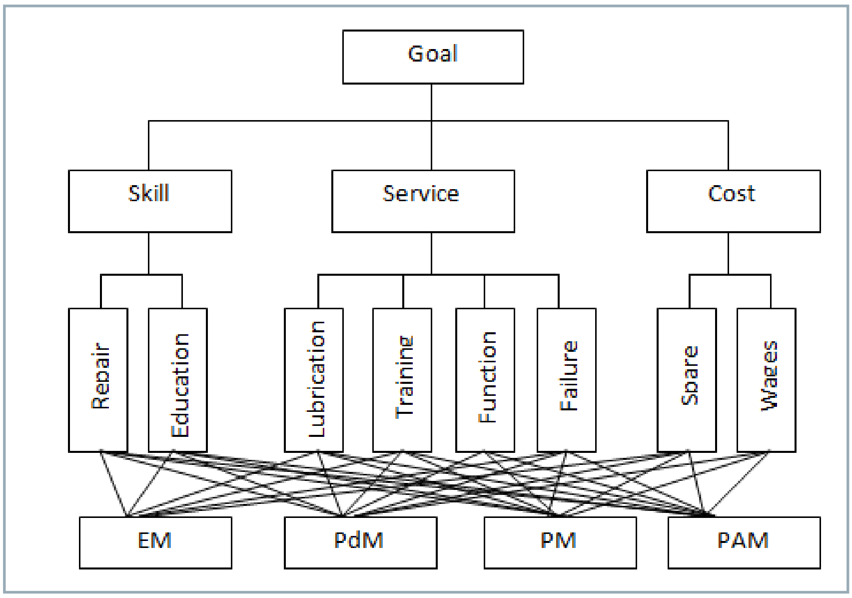

Fig. 2 Flowchart of AHP for selection of the best maintenance strategy

breakdown of the parameters allocated to each factor, following results were obtained (Table 5).

In regards to the parameters in each factor, factors are labelled. They were called respectively; factor 1 – service, factor 2 – maintain cost, factor 3 – skill.

By determining the purpose and defining the factors in the Expert Choice software, the weight of each factor was determined (Fig. 3).

Considering the weight of factors, service factor is the most important in choosing a maintenance strategy; followed by skill and cost factors. Subsequently, the weight of the factors in the criteria was determined.

Therefore, it can be said that factor 1 has the same effect on the preventive, predictive and proactive strategies that are included in the planned programs, because service is one of the main factors of these three maintenance operations. Also, the weights of factor 2 in emergency maintenance (EM) and factor 3 in proactive maintenance (PAM) are greater. Finally, using the

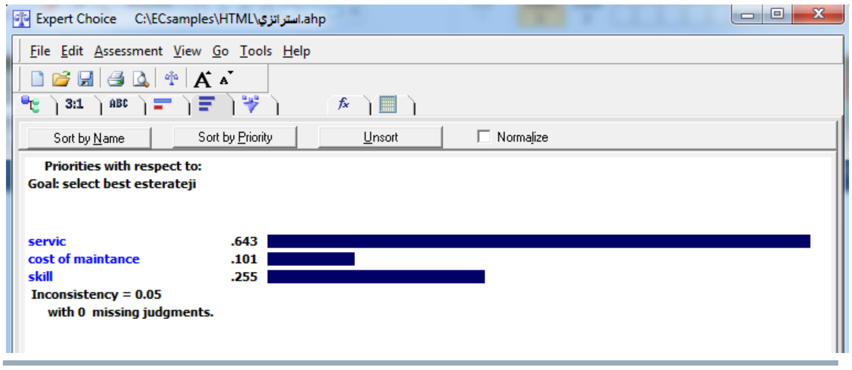

Fig. 3 Weight of each factor

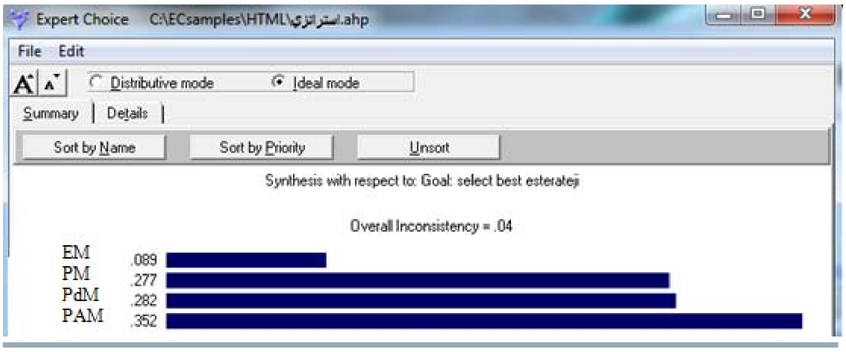

Fig. 4 The final weight of the examined strategies

weight of the factors and the weight of each factor in the criteria, we arrive at the final weight of each of the strategies.

The weight of the preventive, predictive, and proactive strategies is close, due to the alignment of the goals of these strategies that are almost complementary to each other. However, as the proactive strategies (PAM) attempt to root out causes of failures, they are preferable to the others, as was confirmed by calculations and studies. Therefore, the proactive strategy is chosen as the most appropriate. According to Javadian and Hashemi (2013), proactive strategy is actually a combination of preventive and predictive strategies aimed at improving the operating conditions of machines, reducing their need for implementation of the program and completely eliminating the causes of failures.

Conclusions

In this paper, firstly, by combining factor analysis and AHP, factors essential for tractor maintenance were identified. With design of the hierarchical analysis tree, options were evaluated and finally a maintenance strategy was selected. Particularly, results indicate that a push towards modernization of maintenance strategies in the Urmia region is necessary.

In order to be certain of the superiority of the proactive approach to preventive, predictive and emergency methods, it is essential that each of these management systems are applied in the Urmia region so that the results of the paper can be compared statistically with empirical data.

References

AFSHARNIA, F. – ASOODAR, M. A. – ABDSHAHI A. 2013. Regression analysis and modeling of failure rate and its effective factors on tractors in some cities of Khuzestan province. In Journal of Agricultural Engineering, vol. 36, no. 2, pp. 58–49.

BARTHOLOMEW, L. 1981. Farm machinery costing under inflation. In Transaction of ASAE, vol. 24, no. 1, pp. 98–101.

BEHZAD, M. – GHASEMI, A. – EBRAHIMI, A. – ROUHANI A. 2007. Preventive maintenance at water pumping stations. In W. W. C. E., vol. 58, pp. 10–18.

DAHUNSI, O. A. 2008. Spectrometric Oil Analysis – an Untapped Resource for Condition Monitoring. Mechanical Engineering Department, Federal University of Technology Akuer, Undo State, Nigeria.

EXNER, K. – SCHNURMCHER, C. – ADOLPHY, S. – STARK, R. 2017. Proactive maintenance as success factor for use-oriented Product-Service Systems. In Procedia CIRP 64, pp. 330–335.

JAFARI, K. – MAHVI DIANI, M. 2003. A survey on tractor exploitation pattern in Kerman province. In Quarterly Journal of Agricultural Economics and Development, vol. 37, pp. 25–31.

JAVADIAN, M. – HASHEMI, M. 2013. Proactive maintenance for metal molds based on multiplication. In Engineering & Manufacturing Journal, vol. 25, pp. 209–213.

KHODABAKHSHIAN KARGAR, R. – SHAKERI, M. – BARADRAN, J. 2008. Preventive maintenance engineering and monitoring of the situation in road construction machines. In 5th International Conference on Maintenance. Iran Maintenance and Maintenance Association. Tehran.

MIRZAKHANI, H. 2004. Performance analysis of storage planning system in Khuzestan Cement Company. Available at: http://dpe.ir

MOUSAVI POUR, A. – SHEIKH DAVOODI, M. J. – GHANIAN, M. – SAEEDI, N. 2012. Economical comparison of usually urgent oil check and oil monitoring methods for repair and maintenance of sugarcane harvesters. In Journal of Agricultural Engineering, vol. 35, no. 1, pp. 15–27.

RICHARDS, L. 1983. Factor Analysis. 2nd Edition. Lawrence Erlbaum Associate Inc.

SAY, S. M. – SUMER, S. K. 2011. Failure rate analysis of cereal combined drills. In African Journal of Agricultural Research, vol. 6, pp. 1322–1329.

SHIRMOHAMMADI, A. 2002. TPM maintenance and repair. 1st Edition, Arkan Inc.

ZASADZIEŃ, M. – MIDOR, K. 2018. Statistical process control as a failure removal improvement tool. In Acta Technologica Agriculturae, vol. 23, pp. 124–129.

DOI: 10.2478/ata-2019-0004

Acta Technologica Agriculturae 1
Nitra, Slovaca Universitas Agriculturae Nitriae, 2019, pp. 17–21

OPERATIONAL DEGRADATION OF ENGINE OIL IN AGRICULTURAL TECHNOLOGY

Petr DOSTÁL, Jakub ROZLIVKA*, Vojtěch KUMBÁR
Mendel University in Brno, Czech Republic

Proposed paper is focused on description and observation of operational degradation of engine oil in agricultural technology. Engine oil is one of the most important liquids used in combustion engines. Correct function of any machine is based on the appropriate selection of lubricants; moreover, it is also important to care for the entire lubrication system. Determining the condition of the oil used in operational conditions is very important for potential further oil use. Previously, engine oil had to be changed after expiration of legally valid intervals regardless of its actual performance parameters. However, its usage may be extended if engine oil parameters meet the legal requirements. This can be achieved by removing engine oil samples from machines on a regular basis. By examining the samples taken, it is possible to determine the actual oil state. In such manner, it is possible to prolong interchange periods and save both the financial resources and environment.

Keywords: engine oil; oil degradation; metals in engine; viscosity; density

Tractor fluids are used for lubrication of transmissions, final drives, wet brakes, etc. (Kučera and Aleš, 2017). However, these fluids are primarily exposed to heat, chemical and mechanical stress during operation. These kinds of lubricating oil loads are the main cause of its "aging" and contamination. Oil gradually loses its lubricating ability. These penetrate the crankcase of gases between the piston and cylinder, causing oil oxidation. Acids can also be produced. Furthermore, oil is also contaminated by carbon, dust and metal particles. This is due to oil contamination by particles in the combustion chamber and their subsequent combustion (Hromádko, 2011; Kosiba et al., 2016). Impurities and condensing water deteriorate the oil circulation in lubrication system. The heavier components of gasoline, especially in cold engine, dilute the lubricating film on the cylinder wall. Considering the diesel motors, lubricating oil is also contaminated by soot. Contaminated fluid poses a risk to the machine in terms of wear and failure (Tulík et al., 2013). Contamination is very dangerous since it accelerates degradation and oxidation processes in fluids (Tkáč et al., 2017).

Mechanical impurities (dust, carbon, metal particles) can be removed using a suitable cleaner. However, oil degradation caused by chemical influences (oxidation) remains. Application of cleaners can postpone the necessity to change the lubricating oil, but regular replacement of oil is necessary to maintain acceptable engine life. Terms for oil exchange are fixedly determined by manufacturer on the basis of travelled distance or engine operating time.

The main aim of this work is to find out if the oil replacement service interval in agricultural machines can be extended if oil samples are regularly taken for subsequent analysis of important parameters determining whether oils are still suitable for further operation. Motor oil samples were taken from the Zetor 5211 tractor. This tractor is used as a training vehicle of driving school at the Secondary school of Crafts and Services in Velké Meziříčí. Therefore, this machine is operated mostly on road traffic. Tractors of this type are used as training vehicles in driving schools even today. Although it is an older machine, it is represented in great numbers in the Czech Republic. In general, it can be said that Zetor tractors are still the most utilized tractors in the Czech Republic. Motors in the Zetor 5211 tractor are used also in UNC loaders and DESTA lift trucks. Technical parameters of the Zetor 5211: power max – 32 kW/43 hp; displacement – 2,697 ccm/2.7 L/165 cin; cylinders – 3; cooling – water-cooling; fuel capacity – 55 L/15 gal.

Material and methods

Madit M7 ADS III engine oil was used for the measurement purposes. This oil is universal year-long engine oil and suitable especially for heavy freight, ship and rail transportation according to the producer's recommendations. The oil is suitable for over-filled, as well non-over-filled diesel engines. It can be used in agricultural, forestry and earth machines. This oil is used in a mixed fleet and its technical parameters are shown in Table 1.

This oil was taken from the Zetor tractor. Sampling interval was set to be 50 hours of operation. The first oil sample taking was performed after oil replacement and after a short machine operation. Individual samplings are shown in the following table (Table 2). Furthermore, a sample of new unused oil was taken in order to compare it with the

Contact address: Jakub Rozlivka, Mendel University in Brno, Faculty of Agronomy, Department of Technology and Automobile Transport, Zemědělská 1, 613 00 Brno, Czech Republic, e-mail: jakub.rozlivka@mendelu.cz

Table 1 Technical parameters of tested oil

Oil type	Viscosity class	Efficiency class	Kinematic viscosity ($mm^2 \cdot s^{-1}$)	Density ($kg \cdot m^{-3}$)	Pour point (°C)
Madit M7 ADS III	SAE 20W-40	API CF/SF	127.4	899	-30

Table 2 Performance of sampling of oil samples

Sampling date	9. 4. 2016	11. 4. 2016	3. 5. 2016	24. 5. 2016	6. 6. 2016	2. 7. 2016	24. 9. 2016	24. 10. 2016
Meter status (Eh)	870	875	923	979	1,024	1,075	1,125	1,170
Sampling interval (Eh)	0	5	48	56	45	51	50	45
Count per cartridge (Eh)	0	5	53	109	154	205	255	300

Table 3 Measured content of major structural metals in oil

Sampling date	9. 4. 2016	11. 4. 2016	3. 5. 2016	24. 5. 2016	6. 6. 2016	2. 7. 2016	24. 9. 2016	24. 10. 2016
Eh count per cartridge (Eh)	0	5	53	109	154	205	255	300
Al (ppm)	1.41	0.68	3.23	6.91	5.59	8.49	10.78	11.23
Cr (ppm)	0	0	0.11	0.37	0.53	1.16	1.38	1.62
Cu (ppm]	0.31	0.53	1.43	2.6	2.43	3.88	4.25	4.62
Fe (ppm]	0	10.48	15.79	23.8	30.25	56.29	73.47	98.93

default values. All information on these samples is provided in Table 3.

A sample of the oil taken must constitute the average composition of the lubricant used in the machine. It was taken at the engine's operating temperature (minimum oil temperature of 65°C), 3 minutes after stopping the engine at the latest. Sampling was performed using a sampling preparation from an oil tank at 2/3 of its height through a hole for inspection gauge. Oil suction was carried out by means of a plastic suction syringe with an extension adjusted to the needed length. Samplings taken were filled to new plastic sample containers with volume of 50 ml and were filled up to 80% of container volume. There were performed 8 oil takings; 200 ml of engine oil was sucked in each taking. To avoid unwanted contamination and impurities, a new sucking device, previously unused, was used only for sampling from the investigated machine. Samples taken were held in new, dry and clean sample containers that were carefully closed after the sampling. Sample containers were marked and basic data were recorded on them (sampling number, sampling date, operating hours counter status) after taking a sample. The first sampling was performed after engine oil replacement and a short machine operation. Other samples were taken at intervals of 50 hours of operation. However, this interval has not been strictly maintained because the observed tractor was not always at the place suitable for engine oil sampling at the exact time. Seven samples were taken from the tractor oil tank and 1 sampling of new oil in order to compare the measured parameters (Čupera et al., 2010).

Three measuring instruments were used in order to find out the state of the engine oil. Chemical composition of the oils was determined by means of a Spectroil Q100 instrument. In addition to this, Mettler Toledo Densito 30 PX digital density was used for determination of oil density and Anton Paar DV-3P rotational viscometer was used for determination of oil dynamic viscosity.

Oil chemical composition was determined by means of a Spectroil Q100 instrument (a complete semiconductor spectrometer designed for oil sample analysis). This device measures the trace contents of elements dissolved or deposited as fine particles in petroleum minerals or hydraulic mixtures using a long-term proven and reliable rotating disc electrode technique (Kumbár et al., 2012). It meets the requirements of the ASTM D6595 standard method for determination of wear of metals and contaminants used in lubricating oils or hydraulic mixtures (Mettler Toledo.CZ, 2014, Spectro.CZ, 2014).

Density was measured using a portable digital meter Mettler Toledo Densito 30 PX. This device is equipped with a special scale for measuring of petroleum products. It allows determination of sample density in a short time. It uses the oscillating tube method combined with accurate temperature measurement (Ilabo.CZ, 2014).

Anton Paar DV–3P rotational viscometer was used to measure the viscosity. It measures the torque of the rotating swindle immersed in sample. It works on the principle of measuring torsion necessary to overcome the resistance of a rotating cylinder or disc immersed in the measured material. Rotating cylinder or spindle are connected through a spring to a motor shaft rotating at a defined speed. Shaft rotation angle was measured electronically, providing accurate information on shaft or spindle position. Dynamic viscosity value (mPa·s) was displayed on the basis of internal calculation from measured values.

Results and discussion

Substances determined in oil were divided into two groups. The first group involves metals that form the main engine

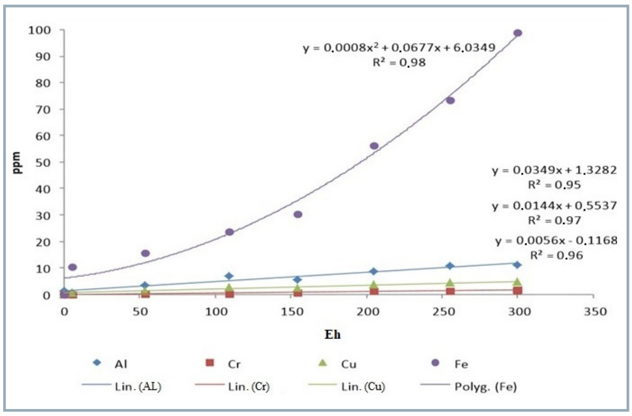

Fig. 1 Increasing metal content in engine oil

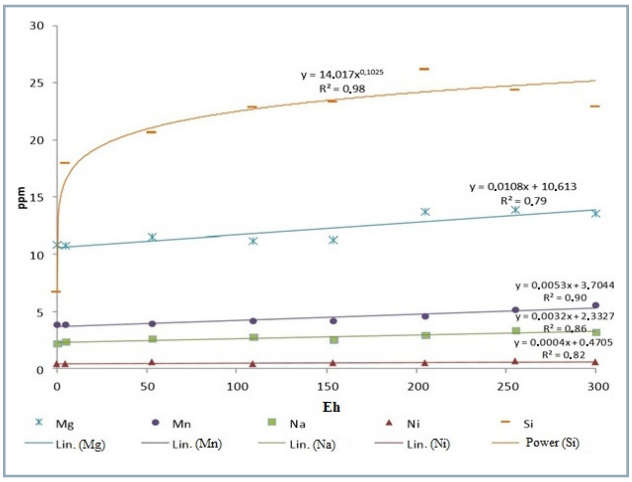

Fig. 2 Content of other metals in oil

constructional parts and the second group includes less important metals. The following tables show the measured values of the amount of main construction metals. Content of individual elements is indicated in ppm.

Considering the Fig. 1, it is obvious that the main construction metal, i.e. Fe is the most present in the samples taken. In comparison to other metals, Fe content in oil is the highest and increase in Fe content is the steepest and most distinct. It can be said that its content grows gradually in case of oil used up to 150 hours of operation. Fe content has almost doubled in the following sample and there was a more distinct increase in the other two samplings. This result may indicate that engine is already more worn and excessive abrasion takes place. Other monitored metals included Al, Cu and Cr. Content of these metals in the samples taken was smaller in comparison to Fe content. In regards to these other metals, Al content was mostly prominent in oil; this is most likely because it is used in larger amounts in engines in comparison with the remaining two. Continuous increase in content of these three metals is gradual and obvious.

The other metals determined in the oil include Mg, Mn, Na and Ni, as well as Si, which, however, is not a construction metal, yet it can be determined in oil analysis. These substances were already contained in a certain amount in the new oil due to additives. As the duration of the tractor operation increased, their content also slightly increased. In regards to this group, Si content was the most prominent in oil. Measured values of individual metals were modelled according to the basic math functions – linear, polynomic (quadratic) and power. Due to these correlations, R2 determination coefficient, value of which determines the suitability of used function, was monitored. Since this coefficient ranged from 0.79 to 0.98, it can be stated that the functions types have been selected accurately (Černý, 2009; Severa et al., 2009). A significant indicator, which can signalise oil depreciation, is density. Density changes due to the operation. Increased lubricant density and its non-consistency impair the quality of lubrication and increase the energy losses due to overcoming of lubricant resistance. Changes in density indicated that oil has been polluted by other substances (Černý, 2007; Oleje.cz, 2014).

Density values gradually increased in the investigated oil. This phenomenon was mainly due to the amount of abrasive particles in oil. Density is affected not only by abrasive metals, but also by other impurities that occur during the operation or they get to the oil from external environment. Therefore, when evaluating the oil state, it is necessary to

Table 4 Measured amount of other metals found in oil

Date of sampling	**9. 4. 2016**	**11. 4. 2016**	**3. 5. 2016**	**24. 5. 2016**	**6. 6. 2016**	**2. 7. 2016**	**24. 9. 2016**	**24. 10. 2016**
Eh count per cartridge (Eh)	0	5	53	109	154	205	255	300
Mg (ppm)	10.83	10.73	11.51	11.18	11.23	13.7	13.87	13.53
Mn (ppm)	3.89	3.83	3.97	4.18	4.17	4.62	5.14	5.54
Na (ppm)	2.25	2.41	2.6	2.76	2.56	2.93	3.34	3.23
Ni (ppm)	0.46	0.47	0.57	0.43	0.55	0.48	0.67	0.56
Si (ppm)	6.73	17.92	20.61	22.84	23.28	26.12	24.37	22.92

Table 5 Measured oil density

Date of sampling	**9. 4. 2016**	**11. 4. 2016**	**3. 5. 2016**	**24. 5. 2016**	**6. 6. 2016**	**2. 7. 2016**	**24. 9. 2016**	**24. 10. 2016**
Eh count per cartridge (Eh)	0	5	53	109	154	205	255	300
Density ($kg \cdot m^{-3}$)	0.8771	0.8782	0.8782	0.8793	0.8798	0.8809	0.8815	0.8826

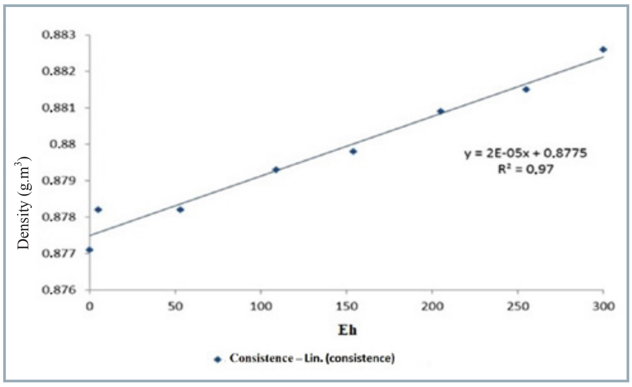

Fig. 3 Measured density values

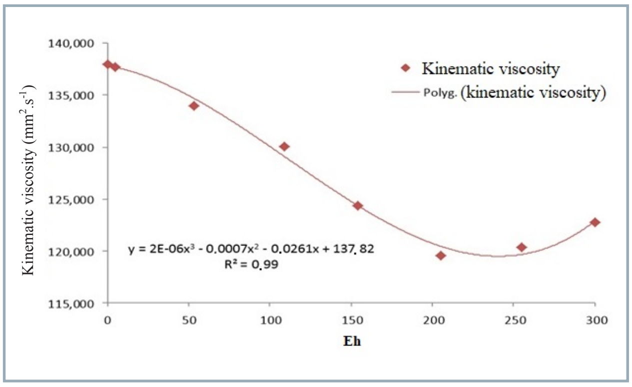

Fig. 4 Dependence of kinematic viscosity on time

Table 6 Breakdown of dynamic viscosity, density and kinematic viscosity

Sampling date	9. 4. 2016	11. 4. 2016	3. 5. 2016	24. 5. 2016	6. 6. 2016	2. 7. 2016	24. 9. 2016	24. 10. 2016
Eh count per cartridge (Eh)	0	5	53	109	154	205	255	300
Dynamic viscosity (mPa·s)	121.018	120.944	117.638	114.348	109.403	105.294	106.103	108.295
Density (g·cm^3)	0.8771	0.8782	0.8782	0.8793	0.8798	0.8809	0.8815	0.8826
Kinematic viscosity	137.975	137.717	133.954	130.045	124.350	119.350	120.366	122.700

pay attention also to this measured quantity, since measured density is used also in calculation of dynamic viscosity and thus directly affects resulting viscosity. Increasing nature of density can be clearly seen in Fig. 4. The first samples taken from the tractor oil tank show almost identical density – there was a slight increase in density in comparison with new oil. Therefore, it can be said that no changes in density occurred in the first quarter of the recommended service interval. Subsequently, density showed increasing trends due to presence of abrasive metals that had just occurred – their content increase more distinctly after 100 hours of operation. Linear function was fitted to the measured values of individual oil samples. The R2 determinant coefficient reached a value of up to 0.97 and thus can be stated that function type was selected appropriately (Kučera and Rousek, 2008; Kumbár et al., 2012; Tulík et al., 2014). Density and dynamic viscosity were measured in tested samples in order to determine the kinematic viscosity. It is one of the essential indicators determining the engine oil state. During trouble-free operation of lubricant in machine, viscosity increases by thickening the oil with impurities and oxidation products; it decreases in the opposite case, e.g. by contamination of lubrication system by fuel or other diluting substances.

In the case of tested oil, kinematic viscosity was gradually decreasing at first as shown in Fig. 4. This phenomenon can be explained especially by mechanic and thermal stresses to which the oil is exposed during operation. Oil degrades due to this reason, i.e. base oil loses its properties, as well as additives represented in oil decrease. If viscosity is too low, mixed to dry friction can occur, resulting in heavy wear and tear, even in engine failure in extreme cases. The lowest viscosity was observed in a sample taken after 200 hours of operation. This corresponds to the normal state when viscosity decreases because of operation. Fig. 4 shows that viscosity has started to increase again in the last two samples taken. This is especially caused by exceeding of recommended replacement interval, when oil is thickened by impurities and abrasive metals. During the operation, oil viscosity should not change by more than ±20%. This requirement has been met and difference between the highest and lowest viscosity amounted to 13.4%. Polynomic (cubic) function was fitted to the kinematic viscosity values of particular oil samples. The R2 determination coefficient reached the value of 0.99 here, thus it can be stated that this function type was selected very appropriately.

Conclusions

On the basis of described measurements, it is possible to state that density values of tested oil in the observed tractor vehicle showed evident increasing trend. This condition was a clear consequence of the increasing amount of abrasive particles in oil.

Kinematic viscosity of oil was gradually decreasing. This was mainly caused by thermal and mechanical stresses to which the oil in engine was exposed to.

After 200 Eh, kinematic viscosity increased due to the increased amount of impurities and abrasive metals in oil. Considering all the measured values, it is highly recommendable that recommended oil change interval should be strictly preserved. This is in compliance with findings published by Sejkorová and Glos (2017), who experimentally observed that it is not advisable to extend change intervals in Zetor tractors. In particular, a number of abrasive metals is already present in oil after 200 Eh, resulting in increased density and also viscosity. Therefore, oil lacks its lubricating properties in comparison to new oil. In such case, it is unnecessary to continuously examine the engine oil state for prolongation service intervals. Observation of these parameters would only make sense merely to determine the engine state, i.e. whether it works properly or shows failures.

On the basis of data found, it is possible to state that continuous engine oil monitoring is not required within one service interval. It should be observed whether the engine operates properly or it has been damaged due to normal degradation and wear of engine oil at service intervals. Tracking of parameters is particularly important in a large fleet, in which oil analysis can be a significant tool for reduction of running costs and prolongation of engine lives. This paper observes a significant problematic in the area of engine oils, bringing new knowledge that can be followed up, if research continues in this field.

Acknowledgement

The research has been supported by the project TP 6/2017: Defectoscopic quality assessment of technical and organic materials; financed by IGA AF MENDELU.

References

ČERNÝ, J. 2007. Engine oil properties – Detergents and dispersants. [on-line], [cit. 2016-2-12]. Available at: <http://www.oleje.cz/clanek/Vlastnosti-motorovych-oleju-Detergenty-a-disperzanty> (In Czech: Vlastnosti motorových olejů – Detergenty a disperzanty).

ČERNÝ, J. 2009. [on-line], [cit. 2016-2-11]. When it says: base oil. Engine oil properties. Available at: <https://www.oleje.cz/clanek/Kdyz-se-rekne-zakladove-oleje> (In Czech: Když se řekne: základové oleje. Vlastnosti motorových olejů).

ČUPERA, J. – SEDLÁK, P. – KARAFIÁT, P. 2010. Differences in rheological profile of diesel and biodiesel fuel. In Acta Universitatis Agriculturae et Silviculturae Mendelianae Brunensis, vol. 68, no. 5, pp. 67–74.

HROMÁDKO, J. 2011. Internal Combustion Engines: A Comprehensive Overview of Issues for All Types of Automotive Schools. 1st ed. Prague: Grada, 2011, 296 pp. ISBN 978-80-2473475-0. (In Czech: Spalovací motory: Komplexní přehled problematiky pro všechny typy technických automobilních škol).

ILABO.CZ. 2014. Densito 30PX. [on-line], [cit. 2016-24-03]. Available at: <http://www.ilabo.cz/produkty/laboratorni-pristroje-opticke/mereni-hustoty/densito-30px/>

KOSIBA, J. – ČORNÁK, Š. – GLOS, J. – JABLONICKÝ, J. – VOZÁROVÁ, V. – PETROVIČ, A. – CSILLAG, J. 2016. Monitoring oil degradation during operating test. In Agronomy Research, vol. 14, no. 5, pp. 1626–1634.

KUČERA, M. – ROUSEK, M. 2008. Evaluation of thermooxidation stability of biodegradable recycled rapeseed-based oil NAPRO-HO. In Research in Agricultural Engineering, vol. 54, no. 4, pp. 163–169.

KUČERA, M. – ALEŠ, Z. 2017. Morphology analysis of friction particles generated in tractor transmission oils. In Acta Technologica Agriculturae, vol. 20, no. 3, pp. 57–62.

KUMBÁR, V. – DOSTÁL, P. – ČUPERA, J. – SABALIAUSKAS, A. 2012. Kinematic viscosity of four-stroke engine oils. In Journal of Young Scientists = Jaunuju Mokslininku Darbai, vol. 36, no. 3, pp. 134–139.

METTLER TOLEDO.CZ. 2014. Densito 30PX. [on-line], [cit. 2016-24-03]. Available at: <http://cs.mt.com/cz/cs/home/products/Laboratory_Analytics_Browse/Density_Family_Browse_main/Portable_density_meter_family_browse_main/Densito_30PX.html>

OLEJE.CZ. 2014. Lubricant additives. [on-line], [cit. 2016-2-25]. Available at: http://www.oleje.cz/clanek/Aditiva_do_maziv (In Czech: Aditiva do maziv).

SEVERA, L. – HAVLÍČEK, M. – KUMBÁR, V. 2009. Temperature dependent kinematic viscosity of different types of engine oils. In Acta Universitatis Agriculturae et Silviculturae Mendelianae Brunensis. vol. 57, no. 4, pp. 95–102.

SEJKOROVÁ, M. – GLOS, J. J. 2017. Analysis of degradation of motor oils used in Zetor tractors. In Acta Universitatis Agriculturae et Silviculture Mendelianae Brunensis, vol. 65, no. 1, pp. 179–187.

SPECTRO.CZ. 2014. Spectroil Q100 – Spectrometer for oil analysis. [on-line], [cit. 2016-24-03]. Available at: <http://www.spectro.cz/store/spectroil-q100-cz.pdf> (In Czech: Spectroil Q100 – Spektometr pro analýzu olejů).

TKÁČ, Z. – ČORŇÁK, Š. – CVIKLOVIČ, V. – KOSIBA, J. – GLOS, J. – JABLONICKÝ, J. – BERNÁT, R. 2017. Research of biodegradable fluid impacts on operation of tractor hydraulic system. In Acta Technologica Agriculturae, vol. 20, no. 2, pp. 42–45.

TULÍK, J. – HUJO, Ľ. – STANČÍK, B. – ŠEVČÍK, P. 2013. Research of new ecological oil-based fluid. In Journal of Central European Agriculture, vol. 14, no. 4, pp. 1384–1393.

TULÍK, J. – KOSIBA, J. – STANČÍK, B. – ŠTULAJTER, I. 2014. Pollution analysis of new synthetic biodegradable fluid during durability test of hydrostatic pumps. In Acta Technologica Agriculturae, vol. 17, no. 1, pp. 24–28.

DOI: 10.2478/ata-2019-0005

Acta Technologica Agriculturae 1
Nitra, Slovaca Universitas Agriculturae Nitriae, 2019, pp. 22–30

MORTALITY OF BROILER CHICKENS DURING SUMMER FATTENING PERIODS AFFECTED BY MICROCLIMATIC CONDITIONS

Veronika ŠRANKOVÁ[1]*, Jana LENDELOVÁ[1], Štefan MIHINA[1], Miroslav ŽITŇÁK[1], Gregorz Nawalany[2]

[1]Slovak University of Agriculture in Nitra, Slovak Republic
[2]University of Agriculture in Krakow, Poland

Mortality of chickens during two summer fattening periods *L*1 and *L*2 in commonly used halls for chicken fattening in Slovakia have been evaluated in this paper. Effect of microclimatic conditions in housing area on recorded mortality has been analysed. Mortality was assessed in six halls, microclimate parameters and surface temperatures were continually measured only in one of the middle halls. It was documented that high mortality occurred during summer in the last phase (P3) of fattening period due to sudden hot weather waves. Daily mortality rate varied up to 447 birds in evaluated hall 3. During the last third of both fattening periods, it was significantly higher than during the first two phases (P_{L1} = 0.0036; P_{L2} = $1.4 \cdot 10^{-6}$). Differences among halls were insignificant (P_{L1} = 0.614; P_{L2} = 0.413). In *L*1, average daily temperatures went beyond the recommended temperatures from 21st to 31st day. During *L*2, it was from 29th to 31st day and from 36th to 38th. The extra high mortality occurred in *L*1 on 31st day (447 birds) and during *L*2 on 36th day (88 birds), 37th day (96 birds) and 38th day (155 birds). High differential temperatures have been recorded and uninterrupted time periods (6 hours or more) with temperature higher than 30 °C and/or the relative humidity (*RH*) exceeding 70% were occurred during these days. In order to eliminate effect of sudden hot weather waves, modern digitally controlled microclimate regulation technologies (heat pumps, floor cooling, etc.) can be used, supported by data obtained from detailed microclimate analysis documented in this paper.

Keywords: broiler chicken housing; mortality; microclimate

With a changing climate, there is an increasing trend in occurrence of extreme climatic events such as heat waves that cause losses in livestock production and negatively affect animal welfare (Lin et al., 2006). High outdoor temperatures burden internal climate in many poultry houses (Sax et al., 2012). They cause heat stress to animals, which has a negative effect on their daily gain in weight, feed intake, growth rate, physiological mechanism and health status (Li et al., 2000). Even one day of high heat causes heat shock and thus high broiler mortality (>1.2%) (Vale et al., 2010). Breeding conditions in poultry houses depend on physical (temperature, relative humidity, lighting, ventilation and dust), chemical factors (air composition such as ammonia, carbon dioxide and oxygen) (Kocaman et al., 2005; Liang et al., 2005; Nawalany, 2012), and stocking density (Sorensen et al., 2000; Algers and Berg, 2001; Hall, 2001; Boďo and Gálik, 2018). Lower mortality and better production parameters were observed in housing with effective environmental quality control, water mist and forced ventilation or floor heating/cooling system (Okelo et al., 2003; Nawalany et al., 2010). Cordeiro et al. (2011) report that one-day-old chickens have difficulty in maintaining body heat because their thermoregulatory capacity is not well developed. Therefore, young chickens (1 to 14 days old) must be kept in an environment with temperature of approx. 35 °C to maintain a constant body temperature. Cooper and Washburn (1998) stated that as chickens grow, they are more vulnerable to high temperatures. According to Thiele and Pottgüter (2008), optimal temperature for adult chickens is 18 °C. Air temperature exceeding 32 °C is considered stressful. Optimal relative humidity in the poultry houses should range between 50% and 70%. If relative humidity falls below the recommended levels, mortality may increase and respiratory diseases may occur in some cases (Czarick and Farichild, 2012). If relative humidity rises above 70%, excessive body heat is drained poorly and air quality is rapidly decreased (Xin et al., 2001; Genc and Portier, 2003; Bansal et al., 2012). In regards to temperature and relative humidity, animal welfare is expressed by the temperature and humidity index (*THI*) proposed by Chepete et al. (2005). It is calculated on the basis of dry and wet temperature. Multiple authors (Heier et al., 2002; Yassin et al., 2009; Chou et al., 2004) studied mortality during the first week of fattening in relation to the next weeks in order to propose improvements of chicken welfare. According to the experience from farms at which the measurements were performed, it is known that mortality is significantly affected by extreme climatic changes in summer by sudden warming, causing a critical

Contact address: Veronika Šranková, Slovak University of Agriculture in Nitra, Faculty of Engineering, Department of Building Equipment and Technology Safety, Tr. Andreja Hlinku 2, 949 76 Nitra, Slovak Republic, e-mail: xsrankova@is.uniag.sk

heat load especially during the last days of fattening. That is reason why research proposed is dedicated to this issue.

Aim of the paper is to evaluate the mortality of chickens during the two summer fattening periods and to find out how microclimatic conditions in housing area affect it. Following hypotheses were established:

H1: Increased mortality of broiler chickens occurs at the beginning of a fattening period and also in summer at the end of it, when it is caused by increased temperature and/or relative air humidity.

H2: Increased mortality of broiler chickens at the end of the summer fattening period is the most properly characterized by the average daily air temperature and relative humidity.

H3: Differential temperature (defined by the difference between actual air temperature and required air temperature) better characterizes heat load of the chickens during the last phase of fattening than the average daily temperature.

H4: For accurate identification of the influence of temperature and relative humidity changes on mortality, their daily averages are not sufficient. Their actual values should be evaluated in more detail – at least at hourly intervals.

H5: Floor temperature is lower than air temperature throughout overall fattening.

Material and methods

Measurements were carried out at farm for chicken broilers with 6 identical halls in Southwest Slovakia. The halls are placed side by side with the same pitch of 17 m between them. Chickens (ROSS 308) were housed into all broiler houses at the same time. Housing area of each hall is 10.5 meters wide and 100.6 meters long, with a total maximum capacity of 20,000 broilers. However, there are only as many birds in the hall so that they do not weigh more than 30 kg per 1 square meter at the end of fattening period. Walls and roof of halls are made as sandwich panels with thermal insulation of 50 mm thickness. Concrete floor of 150 mm thickness is laid on a gravel substrate. The halls are disinfected before each fattening period and floor is subsequently covered with a 100–150 mm high chopped straw bed. The air is supplied to the hall by adjustable flaps with dimensions of 530 × 260 mm located along both longitudinal sides of the hall (2 × 44 pcs.). The exchange of air in the breeding area is ensured by five ceiling suction fans with a diameter of 645 mm and a capacity of 13,600 cubic meters per hour. Ventilation in the hall is controlled by the gradual activation of the ceiling fans until the desired internal state of environment is achieved. During the summer season, 3 exhaust fans are also used, each with a diameter of 1,400 mm and a capacity of 36,000 cubic meters per hour. Ventilation is automatically regulated on the basis of temperature and humidity conditions in the housing area. Assessment of mortality and microclimatic parameters took place during two periods in May–June 2016 (*L*1 period) and May–June 2017 (*L*2 period). Fattening period length was 39 days in both cases. Mortality was assessed in all six halls, microclimate parameters and surface temperatures were continually measured only in one of the middle halls (Hall 3). Mortality was recorded daily. Indoor and outdoor microclimate parameters – air temperature and relative humidity were continuously measured throughout the whole fattening periods. Data were recorded at 10 minute intervals via the COMET S 3121 datalogger. On the basis of measured data, average daily values of temperature and relative humidity were calculated. Recommended values for the chickens (Ross 308, 2018) were used as a benchmark. Since the recommended values are set at 3 day intervals, we have set the temperature values at four humidity levels by regression and interpolation for the other days from day 1 to day 27 (Fig. 1).

This allowed to establish daily so-called "Differential temperature", i.e. values that exceeded the recommended temperatures at corresponding relative humidity values. At critical periods of higher mortality, microclimate parameters were analysed at hourly intervals. We have determined the limits of the air temperature (T_{ai}) and the relative air humidity of the given type of housing in Slovak climate zone and calculated the length of exposure of T_{ai} ≥30 °C and *RH* ≥70%. In order to assess the temperature-humidity status of the environment, *THI* was calculated. Since

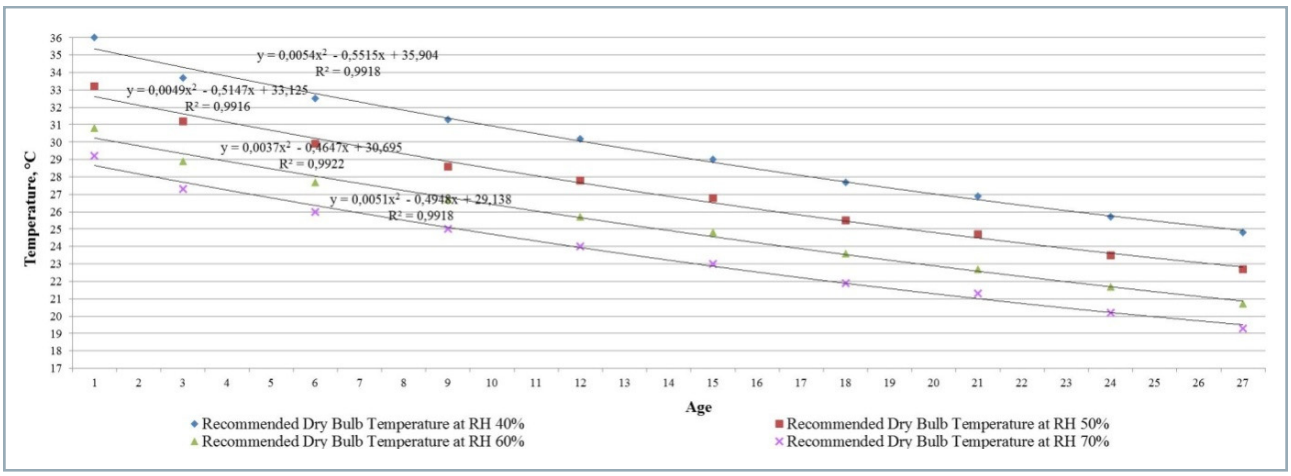

Fig. 1 Recommended air temperature values for 4 relative humidity levels (Ross, 2018) and their adjustment by regression for climate data processing for each day of fattening period

interpretation boundaries of it are not specified for Slovak climatic conditions, method of Chepete et al. (2005) was utilized as follows:

$$THI_{5-6wk} = 0.71T_{db} + 0.29T_{wb} \quad (1)$$

where:
THI_{5-6wk} – temperature-humidity index for the 5th and 6th week of fattening (°C)
T_{db} – dry-bulb temperature (°C)
T_{wb} – wet-bulb temperature (°C)

During both periods *L*1 and *L*2 in the hall 3, the temperature of the straw bed and surface temperature of the concrete floor under the straw bedding were measured using the DS 80 temperature datalogger at intervals of 10 minutes. Mortality and climatic parameters were evaluated statistically during each fattening period using STATISTICA 10 software. For this purpose, fattening periods were divided into 3 equal phases: *P*1 phase – from day 1 to day 13; *P*2 phase – from day 14 to day 26; *P*3 phase – from day 27 to day 39.

Differences between halls and between individual periods in terms of mortality and climatic factors were evaluated by a Multifactor ANOVA; difference significance was determined by Sheffe's test.

Results and discussion

Mortality during fattening period

Total mortality during *L*1 at entire farm was 4,369 birds, representing 4.28% of total number of birds at farm. Daily mortality rate during *L*1 varied from 5 to 702 birds per hall (Fig. 2). During the first fattening week, it was from 6 to 49 birds. Total mortality during whole first week was 121 birds per hall, representing 0.72% of the total number of birds. This is in range of 0–3.3% reported by Yassin et al. (2009). Mortality observed during the first fattening week was also lower than the values of Heier et al. (2002), who evaluated mortality at the beginning of fattening period at different times of the year (1.05% for June).

Average mortality rate during *P*1 phase (1st to 13th day) was 15.31 birds per day and per hall. During *P*2 phase (14th to 26th day), daily mortality was very low and balanced, ranging from 5 to 10 birds per day and per hall; average mortality rate was 7.73 birds per day and per hall. During *P*3 phase (27th to 39th day), daily records continued to show the trend of low mortality with the exception of the 31st day, when chicken mortality increased acutely and ranged in individual halls from 148 to 702. After this event, mortality was low again as during *P*2 until day 39, i.e. until the end of

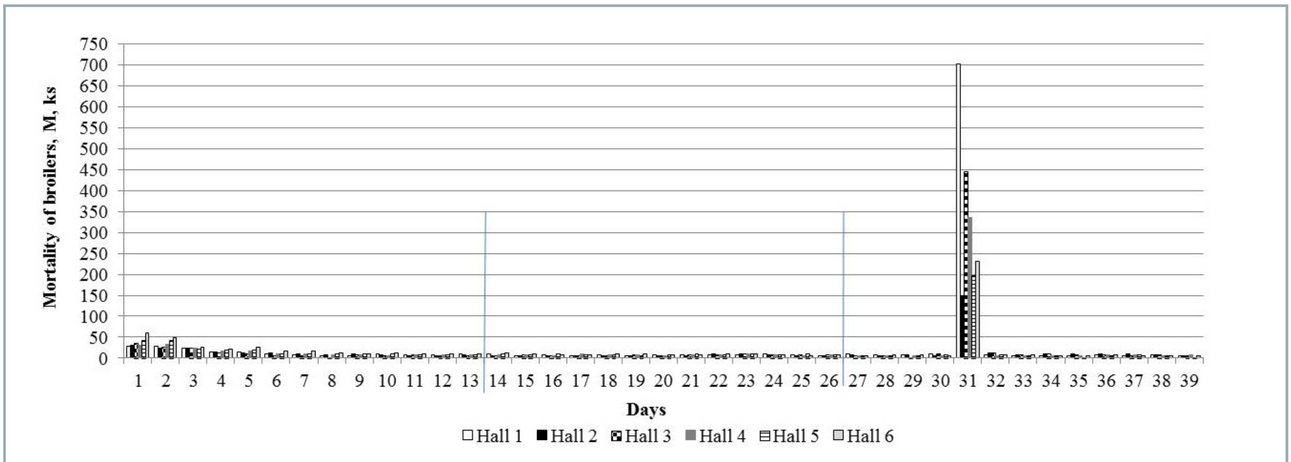

Fig. 2 Daily mortality of broilers in 6 halls during the summer fattening period *L*1

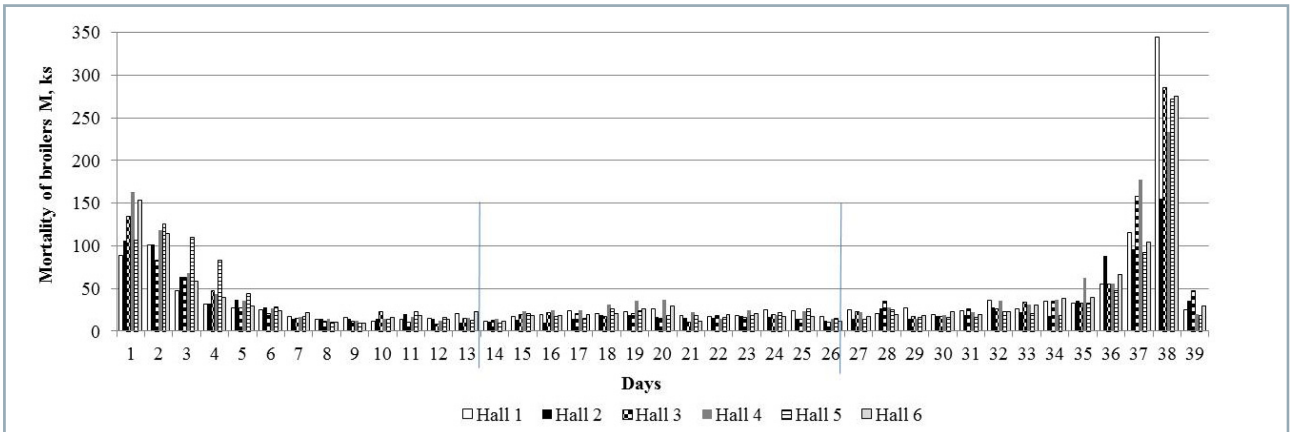

Fig. 3 Daily mortality of broilers in 6 halls during *L*2

Table 1 Results of Multifactor ANOVA of mortality differences among 6 halls and 3 phases of *L*1

ANOVA						
	SS	*df*	*MS*	*F*	*P*-value	*F* crit
Halls*	60,350.9	5	12,070.2	0.7346	0.6141	3.32583
Phases**	340,285	2	170,142	10.355	0.00366	4.10282
Error	164,310	10	16,431			
Total	564,946	17				

* – hall 1, hall 2, hall 3, hall 4, hall 5, hall 6; ** – phase 1 (mortality from day 1 to 13); phase 2 (mortality from day 14 to 26); phase 3 (mortality from day 27 to 39)

Table 2 Results of Multifactor ANOVA of mortality differences among 6 halls and 3 phases of *L*2

ANOVA						
	SS	*df*	*MS*	*F*	*P*-value	*F* crit
Halls*	25,783.6	5	5,156.72	1.11118	0.41305	3.32583
Phases**	642,990	2	321,495	69.2764	1.4E-06	4.10282
Error	46,407.6	10	4,640.76			
Total	715,181	17				

* – hall 1, hall 2, hall 3, hall 4, hall 5, hall 6; ** – phase 1 (mortality from day 1 to 13); phase 2 (mortality from day 14 to 26); phase 3 (mortality from day 27 to 39)

the fattening period. Average mortality rate during *P*3 phase was 32.97 birds per day and per hall.

A statistical comparison showed that the total mortality during *P*3 phase was significantly higher (P_{L1} = 0.0036) than mortality during *P*1 and *P*2 phases (Tab. 1). The differences between the halls were statistically insignificant (*P* = 0.614).

Total mortality during *L*2 at entire farm was 8,783 birds, representing 8.66% of total number of birds at farm. It was more than twice as high as during *L*1. Daily mortality rate during *L*2 varied from 10 to 155 birds per hall (Fig. 3). Daily mortality during period *L*2 in individual halls during the first fattening week ranged from 16 to 163 birds per day and per hall, which was then reduced to an average daily mortality rate of 10 to 19 birds per day and per hall. Total mortality during the entire first week was 377 birds per hall, representing 2.22% of total number of birds per hall. It is more than in *L*1; however, it is still in the range of 0–3.3% reported by Yassin et al. (2009) for first 7 days. In comparison with the results of Heier et al. (2002), we observed higher mortality.

The average death rate for the phase *P*1 was 39.42 birds per day and per hall. In the phase *P*2 it was 18.99 birds per day and per hall. During *P*3 phase, daily mortality ranged from 14 to 345 birds per day and per hall with higher mortality during the last week of the batch. Average mortality rate during *P*3 phase was 54.32 birds per day and per hall. Furthermore, total mortality during *P*3 phase was significantly higher than the mortality during *P*1 and *P*2 phases ($P_{L2} = 1.4 \cdot 10^{-6}$) during this fattening period and differences between the halls were statistically insignificant (*P* = 0.413), (Tab. 2).

Average daily microclimatic parameters

As no bacteriological infections or diseases have occurred at the farm during the observed periods, it is assumed

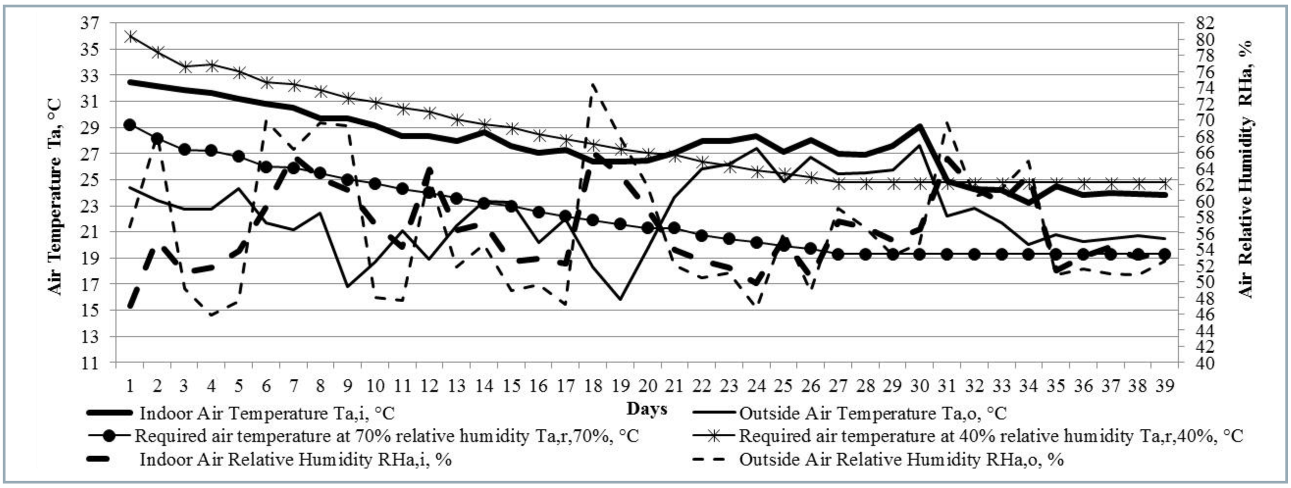

Fig. 4 Daily average indoor and outdoor microclimate parameters during summer for *L*1

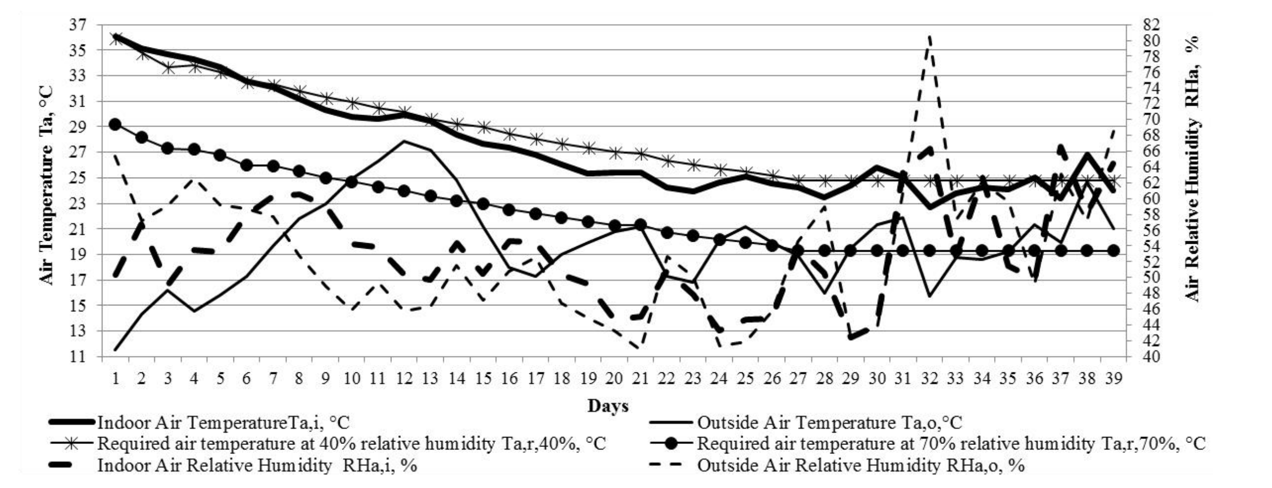

Fig. 5 Daily average indoor and outdoor microclimate parameters during summer for *L*2

that the increase in mortality is caused by changes in the temperature and humidity of the environment during summer. This is in compliance with studies by Teeter et al. (1985), Macari and Furlan (2001), Tao and Xin (2003), Chepete et al. (2005) and Jones et al. (2005), who have showed an importance of average daily temperature in predicting high broiler mortality due to heat stress. Another related study (Li et al., 2000) presented that broiler chickens exposed to heat load will also reduce the daily feed intake. Temperature and relative humidity of the indoor and outdoor air during *L*1 and *L*2 are shown in Figs. 4 and 5, respectively. Average daily indoor air temperatures were higher than outdoor air temperatures during all days of both summer periods. Indoor daily temperature values were almost always going down during *L*1 from 32.4 °C to 23.8 °C and from 36.1 °C to 24.1 °C during *L*2, as the chickens were getting older. However, these were almost always higher than results shown by Vale et al. (2008), who connected the average daily temperature exceeding 24 °C with poor ventilation ($v \leq 1.4$ m·s^{-1}) with and high mortality rate of broiler chickens.

Average daily temperatures during *L*1 went beyond the recommended temperatures set for critical RH = 40% from 21st to 31st day. During *L*2, it was from 29th to 31st day and from 36th to 38th day of fattening period. Especially high mortality occurred during *L*1 on 31st day and on 36th, 37th, 38th days during *L*2. Average outdoor air temperature fluctuated with the minimum temperatures of $T_{a,o,\min,L1}$ = 15.8 °C during *L*1 period, and of $T_{a,o,\min,L2}$ = 11.5 °C during *L*2 and with the maximum temperatures of $T_{a,o,\max,L1}$ = 27.6 °C during *L*1, and of $T_{a,o,\max,L2}$ = 27.9 °C during *L*2. Temperature-humidity index during *L*1 THI_{d30} = 27.12 °C exceeded the critical value of $THI_{crit} \geq 23$ °C published by Vale et al. (2010). *THI* during *L*2 was slightly lower than 23 °C. On the three most critical days of *P*3 phase, *THI* values were THI_{36} = 22.72 °C, THI_{37} = 22.03 °C and THI_{38} = 22.09 °C even though the mortality increased to 155 birds (M_{d36} = 88, M_{d37} = 96, M_{d38} = 155). In both cases of evaluated fattening period, average values of daily temperature and relative humidity were not consistent with the occurrence of death. Atmospheric influx of outdoor hot waves during *L*1 (from 22nd to 31st day) and during *L*2 period (29th to 31st day and 36th to 38th day) were certainly unbearable for animals, yet this was not shown in mortality. We believe that, for this purpose, it would be more evident to use so-called differential temperatures ΔT_v, i.e. values by which the temperature values recommended on the basis of *RH* have been exceeded.

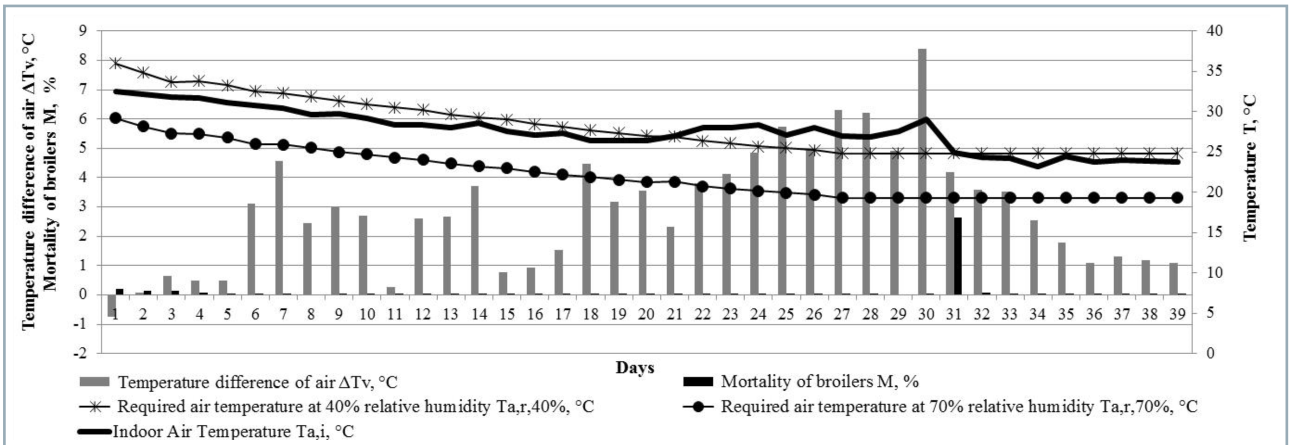

Fig. 6 Daily temperature differences ΔTv, daily mortality $M_{d1\text{-}d39}$ and average daily air temperature T_{ai} in Hall 3 during *L*1

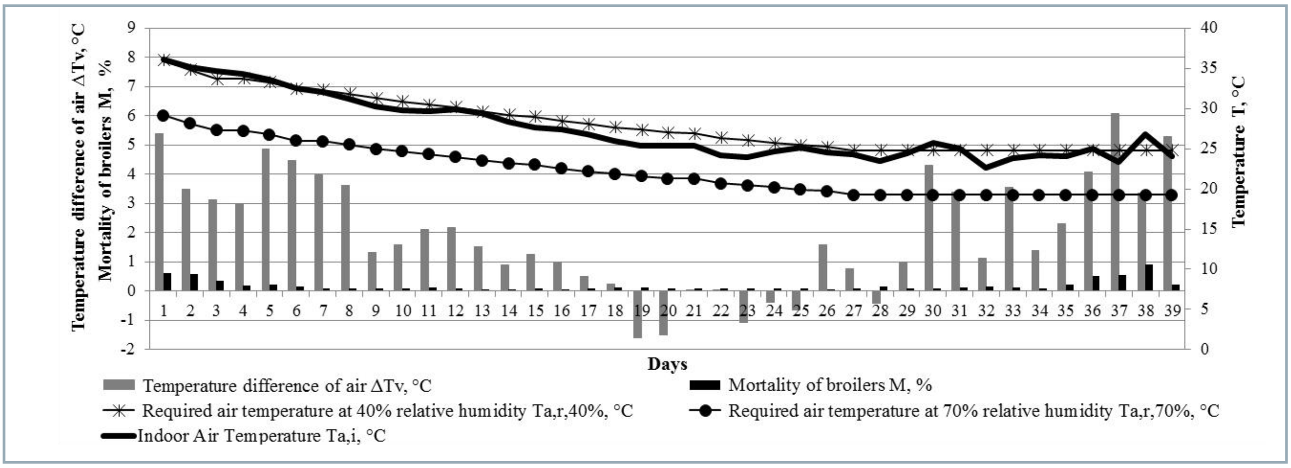

Fig. 7 Daily temperature differences ΔT_v, daily mortality $M_{d1\text{-}d39}$ and average daily air temperature T_{ai} in Hall 3 during $L2$

Differential temperatures

Resulting temperature differences between the actual measured and recommended temperatures during $L1$ and $L2$ are shown in Figs. 6, respectively. There is shown the percentage of dead animals occurred in Hall 3 on each day. Positive temperature differences during both fattening periods are more sensitive to the animal mortality trend, as they also take into account the relative humidity status of each day. At 30th day $L1$, the highest indoor temperature difference was recorded $\Delta T_{v,d30}$ = 8.4 °C, followed by a large increase in mortality M_{d31} = 447. During $L2$, heat spike began earlier, on 29th day. There was also a sudden exceedance of the recommended temperature range at 30th and 31th day ($\Delta T_{v,d30}$ = 4.3 °C; $\Delta T_{v,d31}$ = 3.4 °C), however, mortality did not increase. On 36th and 37th days, ΔT_v suddenly increased again with increase in mortality. The highest animal mortality occurred on 38th day of chickens fattening, which, if disease excluded, could be associated with an increase in indoor air temperature differences $\Delta T_{v,d36}$ = 4.1 °C; $\Delta T_{v,d37}$ = 6.1 °C.

Although the differential temperature assessment was more accurate than average daily temperatures, it was observed that animals were able to adapt to microclimatic conditions and no increase in mortality was recorded at $\Delta T_{v,d27}$ = 6.3 °C and $\Delta T_{v,d28}$ = 6.2 °C during $L1$. On the other hand, acute deaths occurs under less demanding conditions at $\Delta T_{v,d36}$ = 4.1 °C and $\Delta T_{v,d37}$ = 6.1 °C during $L2$. Solution to this issue could lie in analysis of more critical days at shorter intervals.

Evaluation of critical days through average hourly microclimate parameters

It was observed that during the 30th and 31st day of the fattening period $L1$ with average daily indoor temperatures 29.1 °C and 24.9 °C, there was hourly recorded temperature higher than 30 °C for more than 10 hours (from 9:50 to 20:00) (Fig. 8). In afternoon of 30th day, temperature exceeded 32 °C from 11:00 AM to 6:00 PM and it exceeded 34 °C for more than 2 hours. On 31st day of same fattening period with average daily relative humidity of 65.2%, hourly relative humidity exceeded 70% for more than 6 hours (from 1:00 to 7:20). Such conditions caused the highest animal mortality in the entire fattening period (447 birds, in individual halls the mortality ranged from 248 to 702 birds). This is in compliance with results of previous studies reporting that a temperature of 32 °C (Cooper and Washburn, 1998) is unbearable for chickens.

On the basis of average hourly analysis of data from $L2$, it is possible to conclude that none of internal air temperatures exceeded 30 °C (Fig. 9) on 35th and 36th days, but animal mortality was higher than in $L1$. Average daily

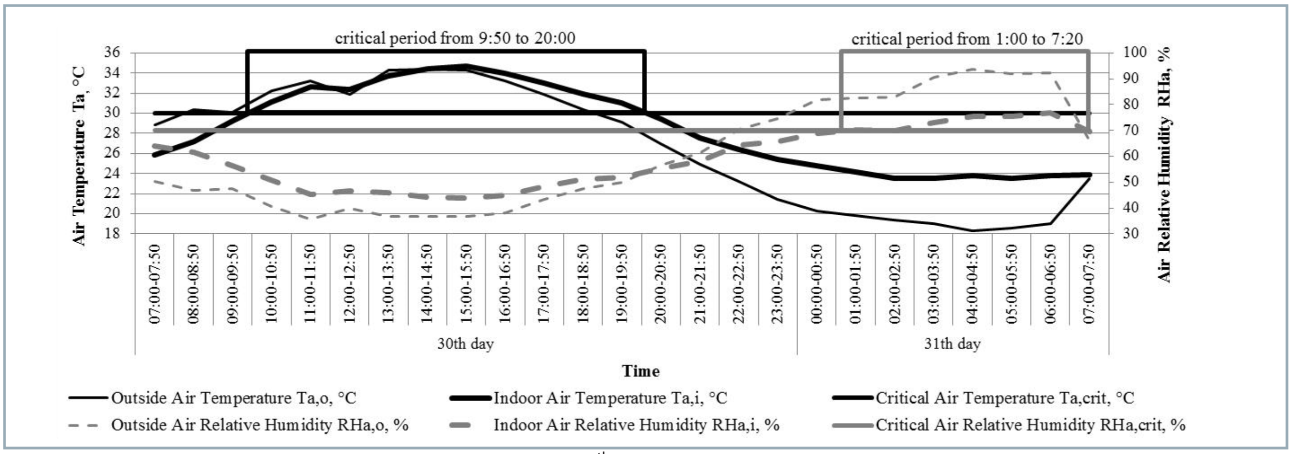

Fig. 8 Average hourly microclimate data during critical 30th day of $L1$, followed by very high acute chicken mortality

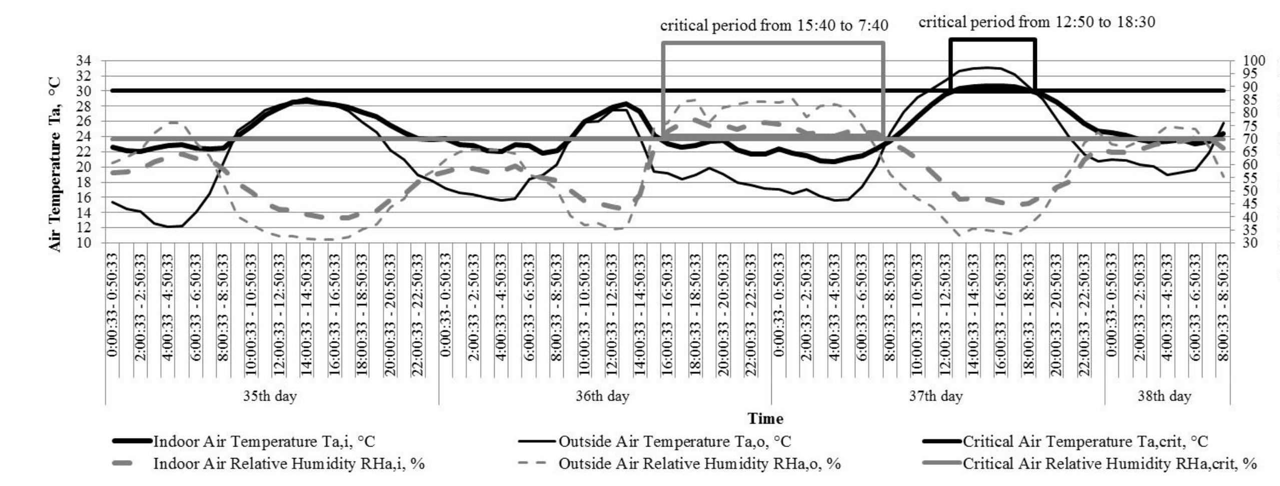

Fig. 9 Average hourly microclimate parameter data during critical time of *L*2

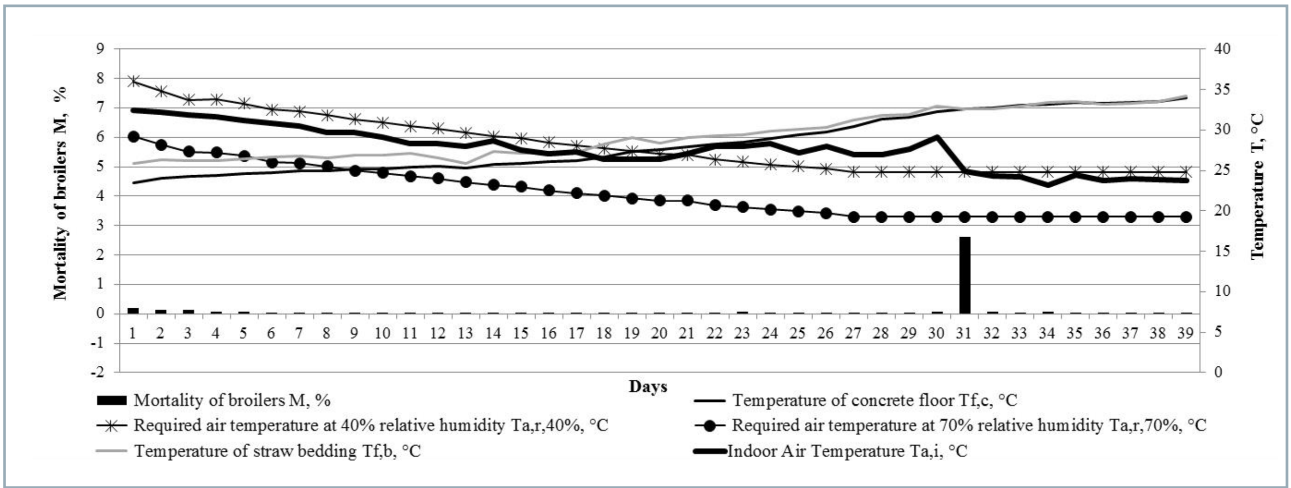

Fig. 10 Results of continuous measurements of temperature of straw bed $T_{f,b}$ and concrete surface temperature $T_{f,c}$ during *L*1 and their comparison to average daily indoor air temperature and required temperature

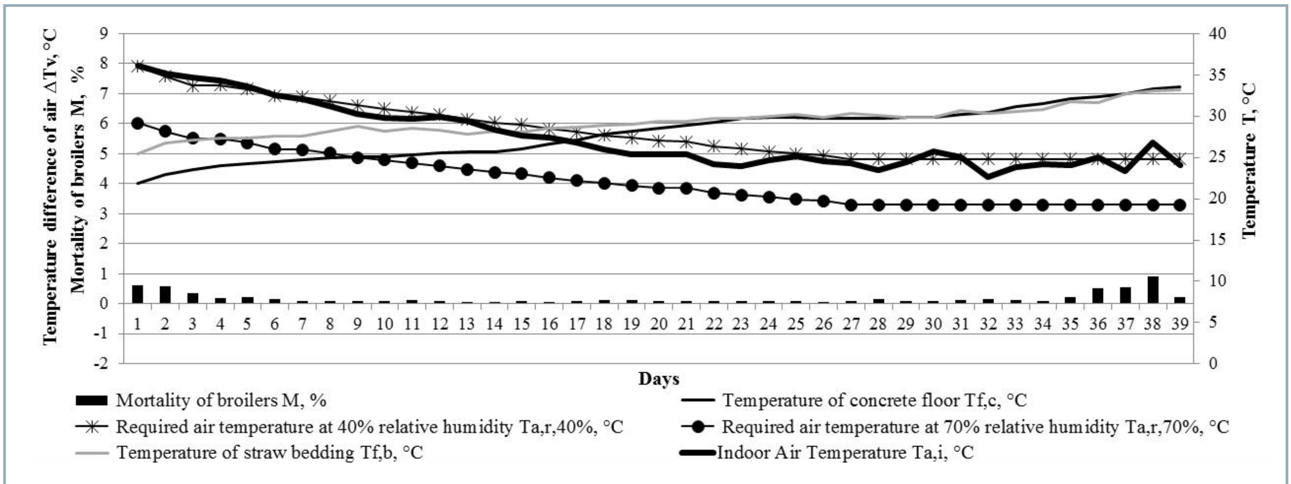

Fig. 11 Results of continuous measurements of concrete surface temperature $T_{f,c}$ and temperature of bed $T_{f,b}$ during *L*2 and their comparison to average daily indoor air temperature and required temperature

indoor air temperature on 35th day was 24.1 °C and it was 25.0 °C on 36th day. However, an increase in the differential temperature ΔT_v began to occur already since the 35th day and it reached $\Delta T_{v,d36} = 4.2$ °C on 36th day and was already $\Delta T_{v,d37} = 6.2$ °C on 37th day. This influence is considered to be significant in relation to high daily mortality on 36th, 37th and 38th days of *L*2 (M_{d36} = 88 birds, M_{d37} = 96 birds, M_{d38} = 155 birds). Simultaneously, we found that during the night before the day of major mortality occurred (36/37 days), relative humidity exceeded 70% for 16 hours (from 15:40 to 7:40), what certainly contributed to increased mortality on 37th day. On 37th day of *L*2, critical indoor air temperature exceeded 30 °C for more than 5 hours (from 12:50 to 18:30). Continuous high temperature on 38th day for 4 hours (15:00 to 18:50) and relative humidity exceeding 70% (6:00 to 7:50) resulted in the highest mortality during *L*2 (M_{d38} = 155 birds).

Floor temperature

On the basis of results from continuous measurements of straw bed temperature during *L*1, it was found that average daily temperature of straw was gradually increasing from the initial temperature of $T_{f,b,d1} = 25.85$ °C to the final value of $T_{f,b,d39} = 34.18$ °C (Fig. 10). Similarly, surface temperature of concrete floor under the straw bedding showed increasing trend (from $T_{f,c,d1} = 23.52$ °C to $T_{f,c,d39} = 34.01$ °C). During period since 18th to final day of L_2, it was found that temperatures of concrete floor and straw bed exceeded recommended ambient temperature and were constantly increasing (min. increase of $\Delta T_{f,c,40\%} = 9.2$ °C and max. increase $\Delta T_{f,c,70\%} = 14.7$ °C). Floor with temperature higher than desired animal ambient temperature (Ross, 2018) at the end of fattening period would certainly not reduce the heat load of birds. Due to warm concrete floors, emitting bedding materials and metabolic heat produced by animals at the end of the fattening period, approximately the same average daily temperature straw (34.18 °C) was reached as in case of concrete floor (34.01 °C). This phenomenon can dangerously contribute to overheating the animals just in the last days of fattening when animals lie on floor for longer time and time of potential conductive share of the form of heat transfer between the body and pad decreases.

Furthermore, temperatures of straw bed concrete floor surface were gradually increasing from $T_{f,b,d1} = 25.49$ °C to $T_{f,b,d39} = 33.2$ °C and from $T_{f,c,d1} = 21.81$ °C to $T_{f,c,d39} = 33.5$ °C during *L*2 (Fig. 11). Since 19th day, both temperatures exceeded the recommended air temperature range; on 39th day of fattening period, temperature of the concrete floor reached a significant increase above the required air temperatures ($\Delta T_{f,c,40\%} = 8.7$ °C and $\Delta T_{f,c,70\%} = 14.2$ °C).

Conclusions

Mortality of chickens during two summer fattening periods in thermally insulated halls frequently used for chicken fattening in Slovakia with a final ventilation intensity of more than 10 cubic meters per hour per bird was evaluated. Effect of microclimatic conditions in housing area on recorded mortality was analysed. Following conclusions can be drawn considering the measurements and analyses:

- Increased mortality occurred at the beginning of fattening periods; however, an acute increase of mortality caused by summer heat spikes occurred when chickens were older than 27 days. The hypothesis H1 was confirmed.
- Mortality did not occur even when average daily temperature exceeded the recommended temperature range. Higher mortality occurred only when differential temperatures were observed to be rising, values of which took into account the relative humidity. Increased mortality generally occurred when differential temperature values were higher than 8 °C. Hypothesis H2 was disproved and hypothesis H3 was confirmed.
- There was rarely a situation when the differential temperature did not exceeded 8 °C yet occurrence of increased mortality was recorded. This required a detailed analysis of that day. Detailed (hour and minute) microclimate parameter record showed that there were uninterrupted extended time periods (6 hours or more) within 24 hours when the average hourly temperature exceeded 30 °C and/or the relative air humidity exceeded 70%. The hypothesis H4 was confirmed.
- Temperatures of straw bed and concrete floor surface were gradually increasing during both fattening periods up to 34 °C without any significant fluctuation during particular days. Required air temperatures were exceeded since 19th day. High temperatures of straw bed and concrete floor, together with high temperatures and high relative humidity, contributed to increased mortality during critical days. The hypothesis H5 was disproved.
- The *THI* value on critical day of mortality incidence during *L*1 fattening period was much higher than commonly used critical value. On each of critical days during *L*2, it was slightly lower than 23 °C. Due to this reason, it can be recommended to decrease the critical value to 22 °C.

We have documented that high occurrence of mortality in summer during the last phase of broiler fattening period due to sudden hot weather waves. To detect and eliminate their effects, it is not enough to monitor only average daily temperatures. It is necessary to use more detailed methods, as presented in this paper, i.e. differential temperatures and/or temperature and *RH* analysis at hourly intervals at minimum. This will provide possibility to use modern technologies effectively for microclimate regulation in housing (heat pumps, water fog, floor cooling, etc.) with their digitized control supported by a data obtained from detailed analysis.

References

ALGERS, B. – BERG, C. 2001. Monitoring animal welfare on commercial broiler farms in Sweden. In Acta Agriculturae Scandinavica, Section A – Animal Science, vol. 30, pp. 88–92.

BANSAL, V. – MISHRA, R. – AGARWAL, G. – MATHUR, J. 2012. Performance analysis of integrated earth-air-tunnel-evaporative cooling system in hot and dry climate. In Energy and Buildings, 2012, vol. 47, pp. 525–532.

BOĎO, Š. – GÁLIK, R. 2018. Monitoring of litter quality and temperature in breeding of fattening chickens. In Acta Technologica Agriculturae, vol. 21, no. 1, pp. 33–37.

COOPER, M. A. – WASHBURN, K. W. 1998. The relationships of body temperature to weight gain, feed consumption, and feed utilization in broilers under heat stress. In Poultry Science, vol. 77, pp. 237–242.

CORDEIRO, M. B. – TINÔCO, I. F. F. – MESQUITA, F. R. M. – SOUSA, F. C. 2011. Análise de imagens digitais para a avaliação do comportamento de pintainhos de corte. In Engenharia Agrícola, vol. 31, pp. 418–426.

CZARICK, M. – FAIRCHILD, B. 2012. Relative humidity... The best measure of overall poultry house air quality. In Poultry Housing Tips, vol. 24, no. 2, pp. 1–3.

GENC, L. – PORTIER, K. 2003. Sensible and latent heat productions from broilers in laboratory conditions. In Turkish Journal of Veterinary and Animal Sciences, vol. 29, pp. 635–643.

HALL, A. L. 2001. The effect of stocking density on the welfare and behaviour of broiler chickens reared commercially. In Animal Welfare, vol. 10, pp. 23–40.

HEIER, B. T. – HOGASEN, H. R. – JARP, J. 2002. Factors associated with mortality in Norwegian broiler flocks. In Preventive Veterinary Medicine, vol. 53, pp. 147 –157.

CHEPETE, H. J. – CHIMBOMBI, E. – TSHEKO, R. 2005. Production performance and temperature-humidity index of COBB 500 broilers reared in open-sided naturally ventilated houses in Botswana. In Livestock Environment – international symposium 7, pp. 524–535.

CHOU, C. C. – JIANG, D. D. – HUNG, Y. P. 2004. Risk factors for cumulative mortality in broiler chicken flocks in the first week of life in Taiwan. In Brazilian Journal of Poultry Science, vol. 45, pp. 573–577.

JONES, T. A. – DONNELLY, C. A. – STAMP, D. M. 2005. Environmental and management factors affecting the welfare of chickens on commercial farms in the United Kingdom and Denmark stocked at five densities. In Poultry Science, vol. 84, pp. 1155–1165.

KOCAMAN, B. – YAGANOGLU, A. V. – YANAR, M. 2005. Combination of fan ventilation system and spraying of oil-water mixture on the levels of dust and gases in caged layer facilities in Eastern Turkey. In Journal of Applied Animal Research, vol. 27, pp. 109–111.

LI, S. Y. – ZHANG, M. H. – ZHANG, Z. Y. – YAN, S. – DU, R. – WANG, K. L. 2000. Effect of heat stress on performance of broilers and some blood biological and endocrinological variate. In Acta Agricuturae Boreali-Sinica, vol. 15, no. 3, pp. 140–144.

LIANG, Y. – XIN, H. – LI, H. – WHEELER, E. F. – ZAJACZKOWSKI, J. L. – TOPPER, P. A. – GATES, R. S. – CASEY, K. D. – BEHRENDS, B. B. – BURNHAM, D. J. – ZAJACZKOWSKI, F. J. 2005. Ammonia emissions from U. S. laying hen houses in Iowa and Pennsylvania. In Transactions of the ASAE, vol. 48, no. 5, pp. 1927–1941.

LIN, H. – JIAO, H. C. – BUYSE, J. – DECUYPERE, E. 2006. Strategies for prevent heat stress in poultry. In Poultry Science Journal, vol. 62, pp. 71–85.

MACARI, M. – FURLAN, R. L. 2001. Environment science on poultry production under tropical climate. In SILVA, I.J.O. (Ed). Environmental science on poultry production under tropical climate. Piracicaba: FUNEP, 2001, pp. 146–164.

NAWALANY, G. – BIEDA, W. – RADON, J. 2010. Effect of floor heating and cooling of bedding on thermal conditions in the living area of broiler chickens. In Archiv fur Geflugelkunde, vol. 74, no. 2, pp. 98–101.

NAWALANY, G. 2012. A proposal to apply operative temperature for the evaluation of thermal conditions in the broiler living zone. In Archiv fur Geflugelkunde, vol. 76, no 1, pp. 49–54.

OKELO, P. O. – CARR, L. E. – HARRISON, P. C. – DOUGLASS, L. W. – BYRD, V. E. – WABECK, S. W. 2003. Effectivenes of a novel method to reduce heat stress in broilers: A cool roost system. In Transactions of the ASAE, vol. 46, no. 6, pp. 1675–1683.

ROSS Broiler Management Handbook 2018. Aviagen 2018. pp. 1–148.

SAX, M. – CAENEGEM, L. – SCHICK, M. 2012. Optimales stallklima dank wärmerückgewinnungsanlagen auch im sommer. In Agrarforschung Schweiz, vol. 3, no. 9, pp. 428–435.

SORENSEN, P. – SU, G. – KESTIN, S. C. 2000. Effects of age and stocking density on leg weakness in broiler chickens. In Poultry Science, vol. 79, pp. 864–870.

TAO, X. – XIN, H. 2003. Temperature-humidity-velocity index for market-size broilers. In Transactions of the ASAE, Paper N 034037, Nevada, 2003, pp. 1–12.

TEETER, R. G. – SMITH, M. O. – OWENS, F. N. – ARP, S. C. – SANGIAH, S. – BREAZILE, E. 1985. Chronic heat stress and respiratory alkalosis: occurrence and treatment in broiler chicks. In Poultry Science, vol. 64, pp. 1060–1064.

THIELE, H. H. – POTTGÜTER, R. 2008. Management recommendations for laying hens in deep litter, perchery and free range systems. In Lohmman Information, vol. 43, pp. 53–63.

VALE, M. M. – MOURA, D. J. – NÄÄS, I. A. – OLIVEIRA, S. R. M. – RODRIGUES, L. H. A. 2008. Data mining to estimate broiler mortality when exposed to heat wave. In Scientia Agricola, vol. 65, no. 3, pp. 223–229.

VALE, M. M. – MOURA, D. J. – NÄÄS, I. A. – PEREIRA, D. F. 2010. Characterization of heat waves affecting mortality rates of broilers between 29 days and market age. In Brazilian Journal of Poultry Science, vol. 12, no. 4, pp. 279–285.

XIN, H. – BERRY, I. – TABLER, G. T. – COSTELLO, T. 2001. Heat moisture production of poultry and their housing systems: Broilers. In Transaction of the ASAE. Agricultural and Biosystems Engineering, vol. 44, no. 6, pp. 1851–1857.

YASSIN, H. – VELTHUIS, A. G. J. – BOERJAN, M. – RIEL, J. 2009. Field study on broilers' first-week mortality. In Poultry Science, vol. 88, pp. 798–804.

DOI: 10.2478/ata-2019-0006

Acta Technologica Agriculturae 1
Nitra, Slovaca Universitas Agriculturae Nitriae, 2019, pp. 31–37

VIRTUAL MODELLING AND LABORATORY RESEARCH OF PARAMETERS OF PLANTING UNIT'S WORKING PARTS

Vladimir Viktorovich KOSOLAPOV[1]*, Elena Valentinovna KOSOLAPOVA[1], Denis Nikolaevich IGOSHIN[1], Anatoly Nikolaevich SKOROKHODOV[2], Alexander Alekseevich RUDENKO[3]

[1]Nizhny Novgorod State University of Engineering and Economics; Knyaginino; Nizhny Novgorod Region; Russia
[2]Russian State Agrarian University – Moscow Timiryazev Agricultural Academy; Moscow; Russia
[3]Togliatti State University; Togliatti; Samara Region; Russia

Research relevance is determined by the need of agricultural producers of Nizhny Novgorod Region to increase the profitability of sugar beet cultivation and to reduce seed losses at sowing. Another important factor is optimal energy efficiency of sowing machines, which can be achieved by reducing the draft force input required to operate the working parts. Leading approach to the research of this issue is to conduct a multifactorial laboratory experiment, taking into account several factors that have the greatest influence on the process of interaction of working parts with the soil. Virtual simulation methods were applied with use of Computer-Aided Engineering (CAE) FlowVision®(TESIS Group) engineering analysis system, allowing creation of close-to-real controlled conditions. Relationships between the lift angle and the span angle of a duckfoot opener were identified; influence of soil moisture content, speed of working parts and their working depth on draft force input and quality of the formed seedbed was determined with justification of their optimal combination. Presented technology and the planting unit assure the technological process quality, they are of practical value for agricultural and engineering companies, as well as for research institutes for design of modern agricultural machinery.

Keywords: virtual simulation; planting unit; laboratory research; energy saving; planter

Increasing crop yields is a priority task in the general paradigm of increasing the profitability of agro-industrial production. This indicator is mainly influenced by the quality of sowing operations, technological operations and machinery involved in the process. It is important to place seeds at the boundary of two soil layers: the lower wet layer to ensure faster root emergence, and the upper loosened layer for supplying oxygen and moisture volatility reduction.

During surveys made in six different fields of Nizhny Novgorod Region during sugar beet sowing, it was revealed that up to 8% of sown seeds remained unburied. This is primarily due to poor quality of pre-sowing soil tillage and imperfection of working parts of sowing machines. In this context, there was a need to develop a seed sowing technology and a plating unit for independent furrowing with subsequent creation of seedbed with densified bottom and walls to ensure an increase in sowing precision. Furthermore, the unit should loosen the lifted soil layer and then lay it back into operating space.

Improving the quality of sugar beet sowing and reducing its energy costs at the same time is an actual problem.

Many researchers have been engaged in solving the problem of planting crop seeds to a strictly defined depth. Importance of precision sowing has been closely observed in works by Upadhyaya and Gowda (2017), Azad et al. (2011). Automation of the depth regulation process has been described by Finnish scientists Suomi et al. (2009), who proposed a mechanism for regulation of sowing depth, as well as its gauging system. A group of scientists (Adamchuk et al., 2004) proposed a new machinery design using modern tools to obtain a high qualitative level of operations and to maximize harvest potential.

Sudduth et al. (2003) studied the possibility of using a system of sensors for reading of soil electrical conductivity in order to further improve the sowing quality by determining the agronomic parameters of the processed material (soil). In addition to the precise placement of seeds and high-quality soil preparation, it is necessary to take into account sowing time, which is an important issue according to Benoit et al. (2015).

The issues of profitability increasing of agricultural production have also been considered by multiple scientist (Leea et al., 2010; Suomi and Oksanen, 2015; McBratney et al., 2004; Stone et al., 2008; Skuriatin and Bondarev, 2008).

An equally important role is played by research aimed at improving agro-technical parameters of sugar beet cultivation, speed modes (Ermakov, 2013; Repetov and Ermakov, 2012), sowing depths and precision sowing (Kosolapov et al., 2016), as well as technological modes (Bulgakov et al., 2017).

Contact address: Vladimir Viktorovich Kosolapov, Nizhny Novgorod State University of Engineering and Economics; Oktyabrskaya str., 22a; Knyaginino; 606340; Nizhny Novgorod Region; Russia; e-mail: vladimir.kosolapov@mail.ru

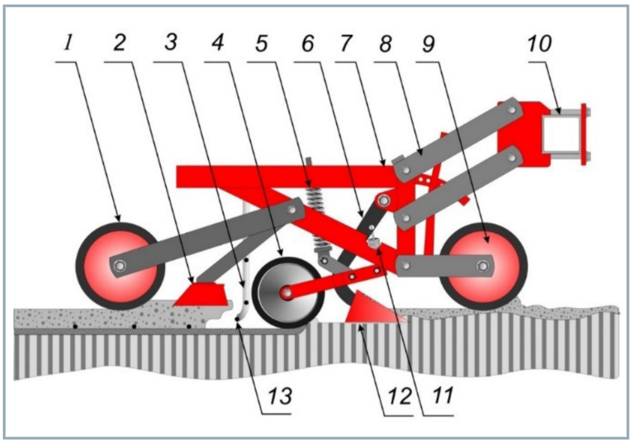

Fig. 1 Design and operation scheme of the planting unit

To improve the quality of sugar beet planting, the authors developed a modernized soil opener mechanism; its novelty is confirmed by a utility model patent no. 118 163 (Kosolapov et al., 2016).

A planting unit (Fig. 1) consists of a frame [7] with the following elements mounted upon it: L-shaped stand [6] with a duckfoot opener [12]; safety spring [5]; press wheel [4] which is pressed against the soil by spring [11]; coverers [2]; packer wheel [1]. Planting depth is adjusted by depth wheel [9]. The unit is fixed to the frame of a drill seeder [10] using a parallel link mechanism [8]. Design of the planting unit can be modified to ensure simultaneous mineral fertilization during sowing (Kosolapov et al., 2016).

Proposed design should provide the sowing technology, novelty of which is confirmed by the patent for invention no. 2494595 Method for Row Crops Planting (Kosolapov et al., 2016), which minimizes the influence of pre-sowing soil preparation quality, and partially relinquishes the use of this operation in the future. Technological process includes: opening the furrow to the base depth (Fig. 2a) – soil is not compacted, but thrown out towards the sides along the row, creating a relatively flat surface without lumps and retaining the capillary structure; formation of the groove up to the sowing depth (Fig. 2b), soil crumbling due to its compacting next to the groove is avoided by densification of its bottom and walls; planting seeds along the groove (Fig. 2c); furrow closing with the loosened layer of soil (Fig. 2d); surface compaction (Fig. 2f) in order to increase the area of seed-to-soil contact.

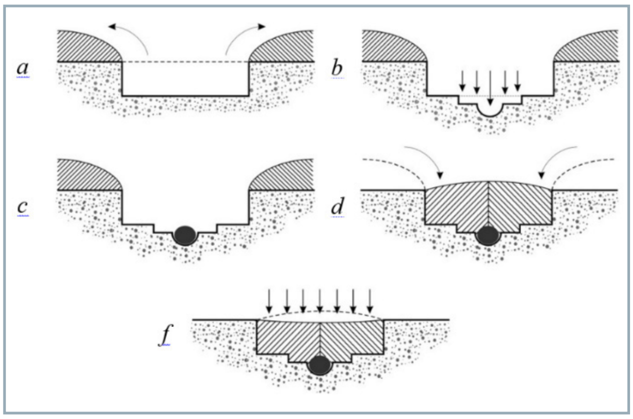

Fig. 2 Seed covering process

Covering of seeds by loosened soil prevents evaporation of moisture and provides seeds with air at the same time, what also has a favourable effect on their germination. Soil under the seeds quickly restores its capillary structure, contributing to early root emergence and an increase in the uniformity of field germination.

In the course of theoretical calculations, geometry variation limits of the planting unit working parts were identified, on the basis of which virtual test models were created (Skorokhodov and Kosolapov, 2013).

In order to confirm theoretical research, as well as to reduce the number of laboratory tests, finite volume method of FlowVision® software package was proposed.

To solve the stated issues, we applied the method of numerical solution to the continuous media dynamics equation presented by Mudarishov et al. (2008).

Advantage of this method lies in the complete isolation of the tested virtual model from external factors with regards to provision of identical conditions for all types of working parts and visual observations in question.

We designed working part models for the planting unit using the SolidWorks® (Dassault Systems) 3D CAD system. According to theoretical calculations, the following wedge face angles faces were subjected to change: angle of crumpling βdf, span angle of the cutting edges γdf, and lift angle (angle of attack) αdf. Kosolapov (2013) showed that pressure exerted on the surface of a dihedral wedge will decrease with decreasing of the aforementioned angles in relation to the seedbed.

Work by Kurdyumov et al. (2015) was taken as a basis for determining the optimal variation limits in the design parameters of the working part, as well as in technological parameters of the medium being treated.

Therefore, we can distinguish the following research objectives:

1. to carry out a virtual research of the designed working part in order to obtain graphical and numerical dependencies of its interaction with the processed environment;
2. to determine optimal geometric parameters of the duckfoot opener with the subsequent manufacturing of the prototype in its actual size;
3. to conduct laboratory tests in order to obtain optimal operating parameters of the unit.

Material and methods

The first research stage is virtual simulation. Process of virtual modelling was carried out using FlowVision® CAE system, in which a design area was completely simulating the actual tillage bin. Designed models were imported into the design area with a possibility to vary the depth of their immersion relative to the separated media, as well as velocity and density of the processed material. We assigned mathematical equations characterizing the considered material, as wells as boundary conditions for the surfaces of the working parts.

For the modelling, subsequent calculation and visualization of the ongoing processes, volume of fluid (VOF) method for tracking the free surface motion was used;

turbulence equations were disabled; vortex, compressibility and surface tension equations were not taken into account (Kosolapov et al., 2016).

A calculation grid consisting of 384,670 cells was superimposed on the design area and model, while the second level adaptation was applied to the boundaries of the working part surface to increase the calculation accuracy of the parameters being read.

As the criteria for assessing the performance of the duckfoot opener, we adopted the parameters that make it possible to obtain a values of the pressure exerted on the surface of the wedge, pressure in the volume of the working medium, trajectories of soil particles, etc. (Fig. 3).

Analysis of the obtained results was carried out using the FlowVision® post-processing software tools, based on the analysis of data created in the super-groups and 'phase volume'-space layers, 'colour contours'-pressure, 'isolines'-pressure, etc.

In this case, main evaluation parameter was the pressure created inside the soil medium and directly exerted on the wedge surface.

Calculation was carried out in a vertical longitudinal section at a distance of 40 mm from the opener line of movement.

For statistical analysis of the results obtained, Portable Statgraphics Centurion® 15.2.11 (Statpoint Technologies, Inc.) software package was used (specifically for calculation of regression coefficients and their significance determination, validity checks of models and plotting of response surfaces).

Before the simulation, an experimental factor matrix was compiled, where x_1 represents the lift angle and x_2 represents the span angle of a duckfoot type furrow opener. We adopted the dynamic pressure P and the quality of seedbed formation K as the optimization criteria.

The second research stage is the laboratory tests. For laboratory research, a prototype of the planting unit with the considered working parts was created.

Laboratory research was carried out using a specialized laboratory installation (Figs. 4a and 4b), which consisted of the bin filled with soil [5], support rails to move the trolley

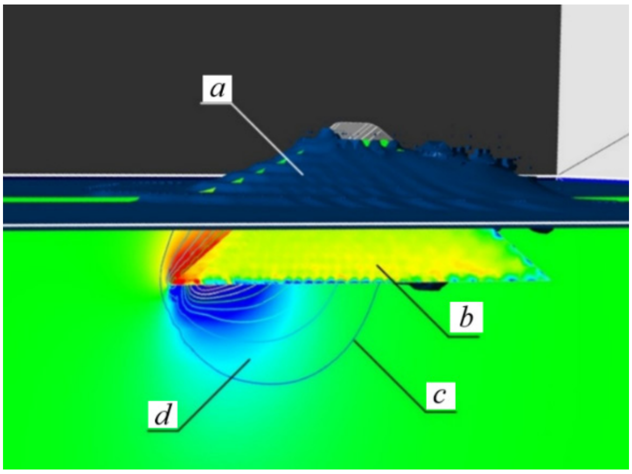

Fig. 3 Calculated parameters
a – motion pattern of particles; b – dynamic pressure on the wedge surface; c – isolines in a horizontal plane; d – pressure produced in the medium in a horizontal plane

Table 1 Experimental factor matrix

Factor	Code number	Variation level		
		-1	0	+1
Lift angle, deg.	X_1	30	45	60
Span angle, deg.	X_2	40	60	80

[8] with the fixed prototype [9]. Trolley was driven by the electric motor [1] through the gearbox [2] and the V-belt drive [3]. When working, the drum [4] winds in the cable [6] connected to the trolley through the dynamometer of DPU type [7].

Physical and mechanical properties of the soil were selected to resemble as close as possible the soil properties of the central part of Nizhny Novgorod Region.

During the laboratory tests, the following parameters were measured: draft force input for the unit; distance covered by the working part; unit speed, depth of the working part; furrow profile, moisture content and density of soil.

The experiments involved: tillage bin – a laboratory installation of the Agricultural Machinery Department of Volgograd State Agrarian University; 1m long metal ruler (according to GOST 427-75 for determining the linear dimensions); boxes (according to GOST 23932 for soil sampling); SHSU drying cabinet for drying samples; electronic scales VST 300/10; SM200 soil moisture sensor

Fig. 4a General view of the laboratory installation

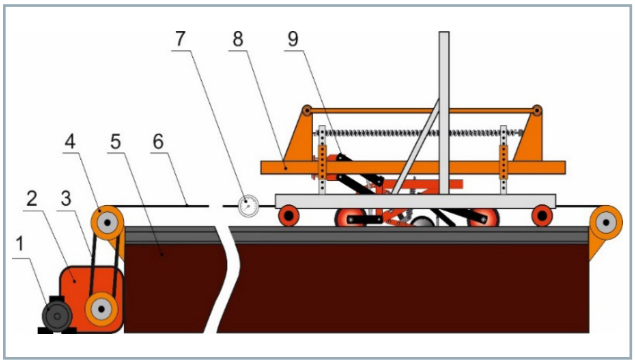

Fig. 4b Scheme of the laboratory installation

produced by Delta-T Devices Ltd. for direct measurement of soil moisture; DPU 5–2 dynamometer for determination of draft force input.

We performed comparative tests of the proposed design of duckfoot type furrow opener with a production version of chisel type furrow opener. For making accurate measurements, proposed duckfoot type furrow opener and the production chisel type furrow opener were alternately placed on the same planting unit (Fig. 5).

During the formation of the sowing bed, the considered working part was to ensure an optimal and uniform planting depth and density of soil at the furrow bottom, as well as to retain soil moisture after the furrow was covered with soil layer.

Technique for planning the experiment was based on Box-Behnken non-positional plan.

To optimize the parameters and operating modes, we adopted the Mathematical Theory of Optimal Experiment.

Based on a priori ranking, the most significant were the following factors:

1. operating speed of the unit v, $m \cdot s^{-1}$, selected limits were limited by the technical capabilities of the laboratory stand – from 2 to 12 $km \cdot h^{-1}$ (from 0.55 to 3.33 $m \cdot s^{-1}$);
2. working depth of planting h, mm, it was selected according to the technological requirements for the cultivation of sugar beet, h = 3–7 cm;
3. soil moisture content W, %, it was selected within the range of 15–35% ± 4%.

The average values of draft force input for the planting unit as the criterion for quality assessment were taken. This criterion is universal and allows for estimation of energy costs that arise during operation of the planting unit, as well as the stability of furrow formation process, estimated by linearity of furrow, and the working depth factor, determining the quality and stability of planting:

$$k_{wdf} = 1 - \left(\frac{h_w - h_m}{h_w} \right) \tag{1}$$

where:

h_w – working depth of planting determined by the depth wheel, m

h_m – actual depth of planting measured after the experiment, m

On the basis of the aforementioned, a matrix of factor variation (Table 2) was created. When using non-composition plans of the second order (Box-Behnken, Hartley, etc.), the factors can be of three levels: upper (+1), main (0) and lower (-1).

Number of experiments, as a rule, is determined by the equation:

$$N = 2^m \tag{2}$$

where:

m – number of factors

In order to obtain regression equations, we used Portable Statgraphics Centurion® 15.2.11.0 software package to process the data. Obtained graphical dependencies were recorded in the form of response surfaces and their 2D cross sections, as well as regression equations corresponding to these surfaces.

Results

On the basis of results from virtual experiment, we obtained regression models describing the influence of the considered factors on the optimization criteria.

In the first case, in determining influence of the factors on pressure, we obtained the following regression equation (with a 95% confidence level) after excluding insignificant coefficients:

$$P = -1{,}569.44 + 14.4444x_1 + 47.5x_2 - 0.481481x_1^2 + \\ + 1.0833x_1x_2 - 0.395833x_2^2 \tag{3}$$

Validity of the obtained R^2 model approximation is 97.49%. For graphical analysis of the regression model, we created a 3D response surface model to determine the influence of the factors on the optimization criterion P. It can be seen that an increase in P criterion occurs with increasing x_1 and x_2 factors, which can be explained by an increase in the vertical component of pressure (Fig. 6).

Analysing the influence of these factors on the unobstructed seedbed optimization criterion with a 95% confidence level, the regression equation can be written as:

Fig. 5 Planting unit with a duckfoot type furrow opener (left) and a production chisel type furrow opener (right)

Table 2 Planning matrix of the factor experiment

Factor	Code number	Variation level		
		-1	0	+1
Speed of the unit *v* ($m \cdot s^{-1}$)	x_3	0.55	1.83	3.33
Soil moisture content *W* (%)	x_4	15	25	35
Working depth of planting *h* (m)	x_5	0.03	0.05	0.07

$$K = -312.714 - 6.42381x_1 - 1.94286x_2 + 0.0384127x_1^2 + \\ + 0.012381x_1x_2 + 0.00535714x_2^2 \quad (4)$$

Validity of the obtained R^2 model approximation is 98.01%. For graphical analysis of the regression model, we created a 3D response surface model to determine the influence of the factors on the optimization criterion K. It can be seen that an increase in *K* criterion, i.e. an increase in the number of particles trapped in the working zone of press wheel, occurs with decreasing x_1 and x_2 factors (Fig. 7).

Visualization and analysis of the processes occurring in the working environment during the duckfoot opener movement were performed along cross sections in vertical and horizontal planes – along the length and height of the opener (Fig. 8).

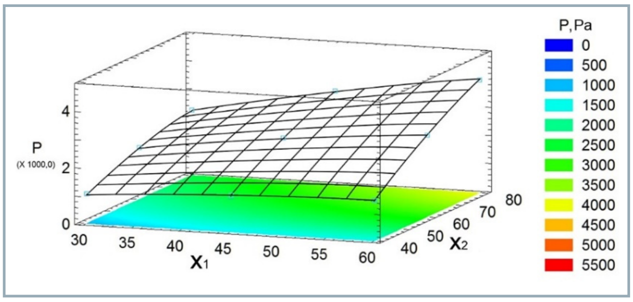

Fig. 6 Relationship of pressure (*P*) versus lift angle (X_1) and span angle (X_2)

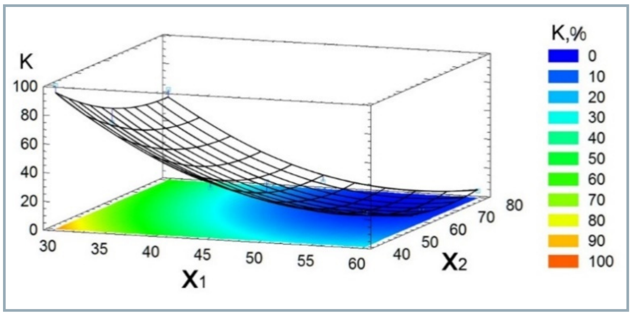

Fig. 7 Relationship of volume of soil particles trapped at the bottom of the furrow versus lift angle (X_1) and span angle (X_2)

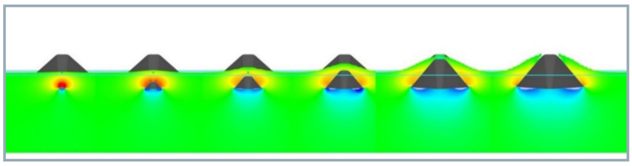

Fig. 8 Scalar field of pressure in the cross sections of the opener

In regards to aforementioned conditions, we selected an acceptable geometry of the opener in question by reducing the received response surfaces to a 2D section of the model (Fig. 9).

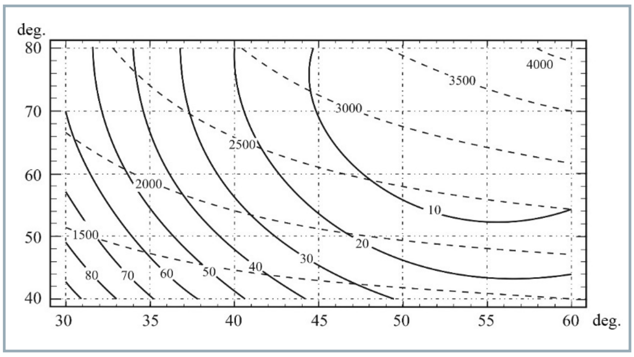

Fig. 9 Combining 2D sections to determine the optimal geometry of the duckfoot opener with required parameters

Fig. 10 Research of the furrow formation process

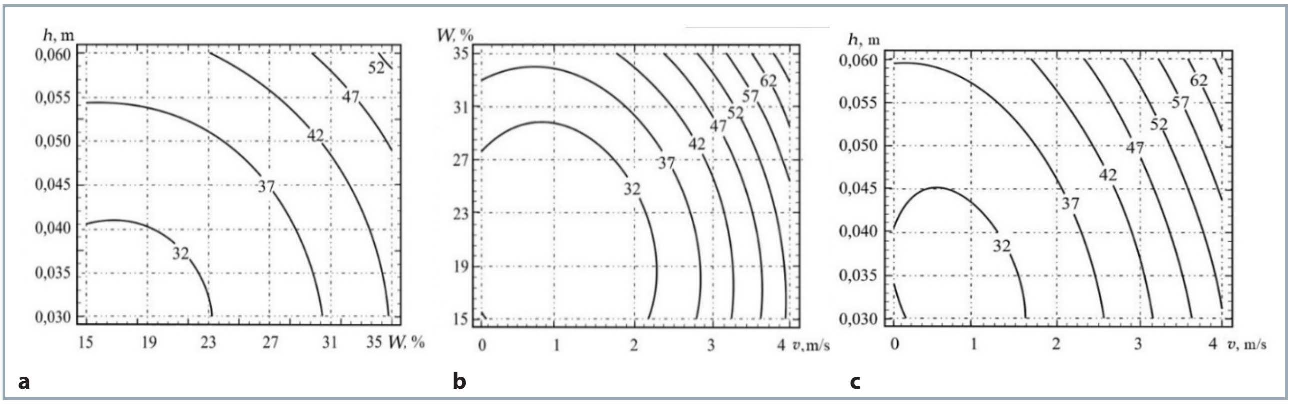

Fig. 11 2D cross-section model depicting the changes of draft force input for the soil opener
a – soil moisture content and depth of planting; b – soil moisture content and speed of planting; c – speed and depth of planting

Results show that the smaller the opener lift angle, the lower the dynamic pressure exerted on its working surface; therefore, at angles of 60° and 80°, the pressure was equal to 3,985 Pa, and at the minimum angles – 1,087 Pa, respectively.

Considering the virtual test results, it is possible to recommend the following values of the considered factors: lift angle (x_1) of 40–45°; span angle (x_2) of 60–70°. In such manner, it is possible to obtain the average pressure value from 2.0 to 2.5 kPa, at which 15–20% of soil particles are trapped at the bottom of the furrow.

Photo and video materials (Fig. 10), as well as numeric data from the measuring equipment were obtained from performed laboratory research.

As a result of the experiments, we obtained graphical representations of influence of the aforementioned factors on draft force input in form of response surfaces, 2D sections, regression equations and their subsequent analysis.

When determining influence of the factors on draft force input, after excluding insignificant coefficients, we obtained (with a 95% confidence level) the following regression equation:

$$R = 25.5639 - 5.82667x_3 - 0.094x_4 - 95.5x_5 + x_3^2 + 0.133333x_3x_4 + 100.0x_3x_5 + 0.0075x_4^2 + 2.5x_4x_5 + 3{,}125.0x_5^2 \quad (5)$$

Coefficient of variation of the obtained regression equation is 0.9249. Analysing the obtained response surfaces (Fig. 11), it is possible to trace an increase in dynamics of draft force input with increasing soil moisture content x_4 and seeding depth x_5, which can be explained by an increase in the coefficient of friction and an increase in the contact area between the wedge working surface and soil. In this case, main influence is stipulated by soil moisture content. A change in the working depth does not significantly influence the draft force input for the working part up to a depth of 0.05 m, but with increasing depth values, the processes characteristic for working parts of subsoil broadcast sowing begin. With an increase in the opener unit working speed over 2.5 m·s^{-1}, there is an increase in the draft force input and in the energy with which soil particles are thrown away from the longitudinal axis of the opener.

Conclusion

Summarizing the research results, we can draw the following conclusions:

1. On the basis of obtained theoretical calculations and results from virtual research, a test piece for the proposed planting unit was created.
2. In terms of results of virtual tests, optimal values for the inclination angles of the duckfoot type furrow opener were obtained. These are: lift angle α_{df} – 40–45°; span angle γ_{df} – 60–70°.
3. We performed laboratory tests, which made it possible to determine relationships of draft force input versus soil moisture content, working depth, and speed. Optimum level of soil moisture content for sowing is within the range of 18–23%. Unit speed at a 23% moisture level should not exceed 2.5–3 m·s^{-1}. With an increase in sowing depth by more than 0.05 m, speed of the planting unit should not exceed 2.0–2.5 m·s^{-1}.

In the course of comparative tests, we observed a 20–25% decrease in draft force input for the proposed duckfoot type furrow opener compared to chisel type furrow opener. This allows utilization of the considered opener in terms of increasing energy efficiency, substantiating the need of its field testing.

Obtained results can be used by agricultural and engineering companies engaged in the production or modernization of planting units, as well as R & D institutes for development of modern agricultural machinery.

The further research will be aimed at increasing the number of regions for possible implementation of the considered unit, taking into account physical and mechanical properties and composition of soils.

It is planned to modernize design of the planting section with inclusion of mechatronic components and automatic soil analysis systems.

Abbreviations

GOST – state standard
SHSU – universal drying cabinet
VST – fixed scales
DPU – universal spring dynamometer

References

ADAMCHUK, V. I – SKOTNIKOV, A. V. – SPEICHINGER, J. D. – KOCHER, M. F. 2004. Development of an instrumented deep-tillage implement for sensing of soil mechanical resistance. In Transaction of the ASAE, vol. 47, no. 6, pp. 1913–1919.

AZAD, Md. S. – MANIK, M. R. – HASAN, Md. S. – MATIN, Md. A. 2011. Effect of different pre-sowing treatments on seed germination percentage and growth performance of *Acacia auriculiformis*. In Journal of Forestry Research, vol. 22, pp. 183–188.

BENOIT, D. – FIEUZAL, R. – RIVERA, M. A. – EZZAHAR, J. – JARLAN, L. – RODRIGUEZ, J. C. – HAGOLLE, O. – WATTS, C. 2015. Impact of sowing date on yield and water use efficiency of wheat analyzed through spatial modeling and Formosat-2 images. In Remote Sensing, vol. 7, pp. 5951–5979.

BULGAKOV, V. – ADAMCHUK, V. – NADYKTO, V. – KYURCHEV, V. – NOZDROVICKÝ, L. 2017. Theoretical consideration of the controllability indicator of machine-tractor unit movement. In Acta Technologica Agriculturae, vol. 20, no. 1, pp. 11–18.

ERMAKOV, V. V. 2013. Results of experimental research on planting sugar beet at various speeds. In Bulletin of Kursk State Agricultural Academy, no. 7, pp. 75–77. (In Russian: Rezul'taty eksperimental'nykh issledovaniy pri poseve sakharnoy svekly na razlichnykh skorostyakh).

KOSOLAPOV, V. V. 2013. Choice and justification of geometric parameters of press wheel. In Bulletin of NNIIE, vol. 24, no. 4. (In Russian: Vybor i obosnovaniye geometricheskikh parametrov prikatyvayushchego borozdoobrazuyushchego kolesa).

KOSOLAPOV, V. V. – KOSOLAPOVA, E. V. – SKOROKHODOV, A. N. – VANDYSHEVA, M. S. – IGOSHIN, D. N. 2016. Development of technology and means for application of mineral fertilizers in sugar beet growing. In Bull. of NGIER, vol. 61, no. 6, pp. 53–59. (In Russian: Razrabotka tekhnologii i sredstva vneseniya mineral'nykh udobreniy pri vozdelyvanii sakharnoy svekly).

KURDYUMOV, V. I. – ZYKIN, E. S. – TATAROV, G. L. 2015. Optimization of parameters and operation modes for multi-level soil opener. In Bulletin of Ulyanovsk State Agricultural Academy, vol. 32, no. 4, pp. 195–200. (In Russian: Optimizatsiya parametrov i rezhimov raboty soshnika dlya raznourovnevogo vyseva semyan i udobreniy).

LEEA, S. – ALCHANATISB, V. – YANGC, C. – HIRAFUJID, M. – MOSHOUE, D. – LI, C. 2010. Sensing technologies for precision specialty crop production. In Computers Electronics in Agriculture, vol. 74, pp. 2–33.

MCBRATNEY, A. – WHELAN, B. – ANCEV, T. 2004. Future directions of precision agriculture. In Precision Agriculture, vol. 6, pp. 7–23. Invited paper, 7th International Conference on Precision Agriculture, Minneapolis, USA.

MUDARISHOV, S. G. – MUFTEYEV, V. G. – MARDANOV, A. R. – FARKHUTDINOV, I. M. 2008. CAD modeling of working surface. In Proceedings of the International Academy of Agrarian Education, no. 7, pp. 37–40. (In Russian: Modelirovaniye rabochey poverkhnosti pluga v SAPR).

REPETOV, A. N. – ERMAKOV, V. V. 2012. Determination of parameters for sugar beet planting unit. In Bulletin of Kursk State Agricultural Academy, vol. 1, no. 1, pp. 118–119. (In Russian: Opredeleniye parametrov agregata dlya poseva sakharnoy svekly).

SKOROKHODOV, A. N. – KOSOLAPOV, V. V. 2013. Theoretical studies of force system exerted on planting unit with modernized soil opener for row crops planting. In XVII International Scientific and Practical Conference of Students and Young Scientists 2013, pp. 20–27. (In Russian: Teoreticheskiye issledovaniya sistemy sil, deystvuyushchikh na posevnuyu sektsiyu s modernizirovannoy soshnikovoy gruppoy dlya poseva propashnykh kul'tur).

SKURIATIN, N. F. – BONDAREV, A. V. 2008. Research of energy-efficient method of planting grain crops. In Polytechnical Network Electronic Scientific Journal of Kuban State Agrarian University, no. 42. pp. 30–44. (In Russian: Izyskaniye energosberegayushchego sposoba poseva zernovykh kul'tur).

STONE, M. L. – BENNEWEIS, R. K. – BERGEIJK, J. VAN. 2008. Evolution of electronics for mobile agricultural equipment. In Transactions of the ASABE, vol. 51, no. 2, pp. 385–390.

SUDDUTH, K. A. – KITCHEN, N. – BOLLERO, G. – BULLOCK, D. 2003. Comparison of electromagnetic induction and direct sensing of soil electrical conductivity. In Agronomy Journal, vol. 95, no. 3, pp. 472–482.

SUOMI, P. – OKSANEN, T. – OJANNE, A. – KALMARI, J. – LINKOLEHTO, R. – TEYE, F. 2009. Automatic working depth control for seed drill using ISO 11783 compatible tractor. In Precision Agriculture 2009 – Papers Presented at the 7th European Conference on Precision Agriculture, ECPA 2009.

SUOMI, P. – OKSANEN, T. 2015. Automatic working depth control for seed drill using ISO 11783 remote control messages. In Computers and Electronics in Agriculture, vol. 116, pp. 30–35.

UPADHYAYA, S. V. – GOWDA, V. V. 2017. A review on agricultural seed sowing. In International Journal of Innovative Research in Science, Engineering and Technology, vol. 6, no. 4, pp. 7216–7223.